



Design, Build and Optimisation of an Accessible Wet Shaking Table for Microplastic Separation from Sediment


MSc Mechanical Engineering
UCL Mechanical Engineering
London WC1E7JE


Abstract

Microplastic pollution in marine environments poses a significant threat to ecosystems, necessitating the development of efficient, low-cost methods for separation and analysis. This study focuses on the design and optimisation of an accessible wet shaking table for separating microplastics from beach and river sediment, which is a known sink for microplastic pollution. A cost-effective prototype is developed using readily available materials and equipment, making it accessible to applications with limited resources. The table is tested and optimised using response surface methodology on spiked beach sediment samples containing known quantities of microplastics, including PP, PE, PS, EPS, PET and PVC. Operational parameters of table inclination, vibration frequency, wash water flow rate, stroke length, stroke frequency and end elevation were systematically adjusted to improve separation efficiency. The table demonstrated up to an 75.3% separation efficiency on artificial sediments, and 59.8% separation efficiency on real sediments during validation. The low-cost design of this wet shaking table presents a valuable tool for microplastics removal, particularly in resource-limited settings.

Keywords: Gravity separation, Microplastics, Plastic pollution, Response Surface Methodology, Sediment, Shaking table

1 INTRODUCTION

In 2019, it was estimated that 460 million tonnes of plastic was produced across the world, marking a more-than-double increase in plastic production across the last two decades [1], [2]. Despite governmental regulation, plastic production is expected to rise to 1.2 billion tonnes per year by 2050, signifying a growing waste crisis [3]. The effects of plastic waste is already widely known, and can lead to a series of negative social, environmental and ecological impacts. For example, plastic pollution in coastal marine habitats and beaches have long been detrimental to maritime and tourism industries across the world [4]. Despite this, due to waste mismanagement and leakages, an estimated 1-2 million tonnes of plastic still enter the oceans annually, where they can persist for up to centuries due to longevity-enhancing chemical additives [2], [5].

An especially troublesome category of plastic waste are microplastics, which are defined as plastic waste less than 5mm in diameter [4]. These can derive either from the weathering of larger plastics, or be intentionally produced to be small [6]. Due to their size, they are highly pervasive, being easily transported along waterways where they can disrupt aquatic ecosystems [7]. Recent studies show that although microplastics make up 8% of the Great Pacific garbage patch by mass, they account for 94% (1.8 trillion) of floating plastic pieces in the area [8], [9]. However, microplastics are not only widespread, but also pose health risks to living organisms. Studies have linked microplastic ingestion to organ damage and behavioural changes in marine species, causing population decline [10], [11]. Microplastics carried into land can also reduce soil water retention properties, affecting plant nutrient cycling while also increasing drought risk [12], [13]. Humans are also susceptible to ingestion through contaminated seafood, which may lead to organ damage, cancers, hormone imbalances and neurodegenerative disease over time [14], [15], [16].

As microplastics are buoyant and easily carried by water currents, a common sink is in beaches and riverbanks [17]. An estimated 40 million tonnes of microplastic have accumulated across global shorelines since

1950, such that some heavily polluted beaches comprise up to 3.3% microplastics by weight [18], [19]. Thus, it is evident that microplastic accumulation on shorelines are a major concern, and that effective removal strategies are necessary. On this front, however, there is a lack of solutions which can be both effective and scalable.

Agitative removal methods such as sieving are currently implausible due to microplastics and sediment material being of similar size [20]. In addition, the sheer amount and small size of microplastic waste in sediment disincentivises manual litter-picking [21]. The current method of choice is density separation, where a mix of sediment and microplastics are submerged in a flotation liquid and allowed to settle [21]. Microplastics which float are skimmed and removed from the liquid surface. Although this method can achieve a high separation efficiency, the media required are often ecotoxic and expensive [22]. A novel high-gradient magnetic separation technique was also recently developed, reporting up to 96% recovery from sediment [23]. This method involves tagging plastic particles with magnetic nanoparticles, which enables their subsequent removal via magnetic field. However, its current application is limited to two polymer types, restricting the fraction of extractable microplastics with this approach [23].

It is thus evident that the current microplastic removal methods available lack the scalability and throughput rates required to address the growing number of microplastics in sediment, and new methods should be considered. To address this issue, this report will assess the viability of Wilfley shaking tables, a gravity separation method from the mining industry, in the removal of microplastics from sediments. Shaking tables are among the most efficient forms of gravity separation used in mining, but are yet to be applied to microplastics separation from sediment [24, p. 10], [25]. These consist of an oscillating grooved tabletop, with a thin water film passing across the table perpendicular to motion. The combined agitation of water and oscillation produces the effect of sorting fine particles by density, and has been prevalently used in the mining industry to extract gold from rock ore [25]. However, these tables are typically 2-3 m in size, consisting of a 300 kg steel frame with high costs, reducing accessibility and widespread application [26]. For the purposes of this report, a small-scale, accessible shaking table will be developed and optimised for the separating of microplastics from beach and river sediment.

A vital part of shaking table design is the optimisation of operating parameters. Shaking tables have 6 different parameters, all of which can affect sorting efficacy. Once optimised, a shaking table can see up to 3.7-fold increases in recovery rate [27]. However, with 6 continuous factors, testing all possible values would prove immensely time consuming. Thus, Response Surface Methodology (RSM) will be used to acquire optimised parameters with experimental economy, conducting testing for optimisation on artificially-produced sediment [28]. Optimisation results will then be experimentally validated using real sediment extracted from the River Thames.

2 LITERATURE REVIEW

2.1 Makeup of Beach and River Sediment

As artificial sediment will be used for table optimisation, it is important to understand the compositional profile of beach and river sediments. A representative spectrum of sediment material and microplastics will allow for proper replication of in-field conditions, and yield stronger results during validation. It is also important to identify plastics by polymer type, as plastic properties such as toughness, buoyancy, ecotoxicity can all vary greatly from polymer to polymer [29]. In 2022, a study by the Organisation for Economic Co-operation and Development (OECD) estimated that the most common plastic polymers produced are the following: PP (16.92% of global production), PE (12.1%), PVC (11.2%), PET (5.4%) and PS (4.6%) [30]. However, the ratio of polymers found in plastic waste is likely to vary due to differing product lifespans, use-cases and recyclability [31]. For example, PS, commonly used in packaging, is likely to enter the waste stream much earlier than high-grade PVC plastic found in vehicles or construction [32]. Moreover, polymer ratios found on shorelines is likely to further change due to different buoyancies and capacity for long-distance transport [33]. As such, it is necessary to consult existing studies specifically on shoreline polymer distribution.

In a 2022 study, a quantitative material flow model was used to predict the distribution of six common polymers across the world: low-density polyethylene (LDPE), high-density polyethylene (HDPE), polypropylene (PP), polystyrene (PS), polyvinyl chloride (PVC) and polyethylene terephthalate (PET) [34]. This includes both the net amount of each polymer in the environment, as well as their accumulation across a number of channels including ocean shorelines, freshwater sediments and urban soils. These findings are shown in figure 1 below.

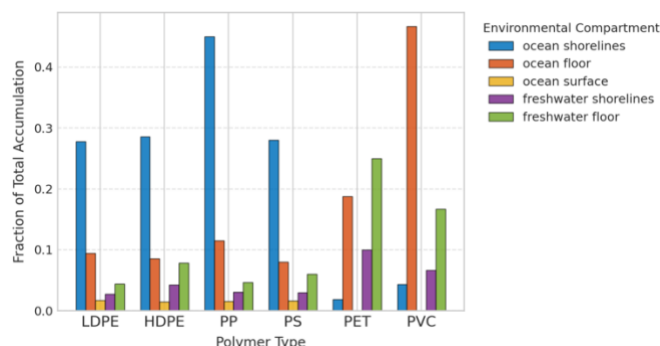


Figure 1: Distribution of Polymers across Environmental Sinks [34]

It is evident from figure 1 that for buoyant polymers like LLDPE, HDPE, PP and PS, ocean shorelines are predicted to be primary sinks. This is reasonable seeing as buoyant plastics have a greater capacity for long-distance transport over water, allowing ocean-bound plastics to eventually wash ashore. Denser plastics, however, like PVC and PET, are non-buoyant and thus are predicted to settle on ocean or freshwater floors. A 2019 study compiled survey data on microplastics found in intertidal beach sediment across the world, validating the model's predictions [35].

In terms of typical microplastic contamination seen in sediments, under normal conditions, microplastics make up tiny fractions, typically below 0.1%. However, due to irregularities in anthropogenic dumping of plastics, microplastics tend to accumulate heavily in specific locations. Kamilo Beach, Hawaii, is estimated to have 5-10% plastic by sediment weight [36].

It is also important to determine the composition of gangue material, i.e. the beach and river sediment to be separated from the microplastics. For beach and river sediment, material is categorised by size using the Udden-Wentworth scale (appendix 6.1). By referring to the scale, for the particle size range in question ($<5\text{mm}$), beach and river sediments are primarily composed of: fine gravel (2-5mm in diameter), sand (0.0625-2mm), and muddy silt (0.0625mm and below).

However, the specific ratio of gravel, sand and silt is difficult to identify, as these depend greatly on factors such as parent rock lithology, mineral compositions as well as chemical make-up which varies by location. Thus, in this section, the target polymers (PET, PVC, PP, PE and PS) are determined, as well as target sediment composition, and the maximum concentration of microplastics present in sediment. These can form the basis on which to develop an artificial sediment sample in section 3.2.

2.2 Existing Methods for Separation of Microplastics from Sediment

Global beach cleanup efforts collectively remove tens of millions of kilograms of plastic each year [37]. Compared to the estimated 6.3 million metric tonnes of cumulative plastic waste on shorelines, it is evident that improvements, or alternative methods are necessary [38].

As previously mentioned, density separation is the current method of choice for microplastic separation from sediment. However, a number of issues are present in the method, which prevents it from being scaled for microplastics removal. The first of which are the required flotation liquids. To facilitate effective density separation, flotation liquids need to be in a density range between that of sediment and the target microplastics [39]. Although lighter polymers like PE, PS and PP ($0.9\text{-}1.1\text{ g cm}^{-3}$) can be removed using cheap and accessible mediums like NaCl (1.2 g cm^{-3}), denser plastics like PVC and PET ($1.38\text{-}1.41\text{ g cm}^{-3}$) require compounds

like ZnCl_2 and NaI for separation, which are ecotoxic and expensive [22]. This would require any recovered sediment to be cleaned before re-entry into the environment. Density separation samples also require 1-2 hours of settling time, which increases in duration with higher volumes of material, reducing scalability [40].

Alternatives to density separation have recently emerged, but at the moment are restricted to niche or limited application. This includes pressurised solvent extraction (PSE), which dissolves organic matter using high-pressure solvents, and extracts microplastics from the resulting sediment matrices [22]. It is particularly effective in recovering smaller particles, outperforming density separation for particles below $150\mu\text{m}$ in diameter. However, the method requires complex and expensive equipment, restricting its application to small-scale laboratory settings [22]. Another is the aforementioned high-gradient magnetic separation (HGMS) method, which is only capable of removing PVCs and PETs [23]. The method also requires ethanol to operate, which may accumulate in the running cost of removal efforts. Another promising novel method is electrostatic separation, which utilises the electrostatic behaviour of plastics to separate them from sediment. Although near 100% separation is achieved for some plastics, variability is seen to be highly dependent on microplastic particle size and thus is not yet entirely effective [41].

Improvements to the density separation method have also been proposed, seeing varying degrees of success. In 2019, Japanese researchers developed the JAMSTEC, a specialised device aiming to streamline the density. It comprises a small glass chamber based on the Utermohl chamber, achieving to 98% microplastic recovery including denser PETs and PVCs using a non-toxic saline solution. However, the device requires grease for lubrication, which was seen to catch some microplastics. In addition, prior diluting of sediments is required if clay is present. A similar device was developed in Germany called the Munich plastics sediment separator. The method was capable of separating plastics with 95.5% efficiency, but only 55% of separated plastics were recoverable. A toxic Zinc Chloride is also used as the separation medium [42].

It is therefore seen that current microplastics removal methods, although effective, benefit targeted applications such as the removal of specific polymers, or small-scale sampling. As it stands, there are no methods offering removal capabilities of all 5 common polymer types (PET, PP, PE, PS, PVC) whilst maintaining reasonable material throughputs and costs without damaging the environment.

2.3 The Wilfley Shaking Table Method

First invented in 1896 by Arthur Wilfley, the Wilfley wet shaking table is typically used to concentrate heavy minerals from the laboratory up to the industrial scale. It consists of a shaking (oscillating) table deck, with a riffled surface. Since its inception, it has been extensively used worldwide and is still used today in mining and metallurgy [43].

Wilfley tables are capable of sorting a wide range of wet and dry materials with an assortment of densities, and as such as often used as secondary sorting methods from previous separation stages [44]. However, these tables are often large, expensive and immobile, as the most common applications are in industry where scale is prioritised over manoeuvrability. Even in laboratory scales, tables typically cost over £5,000, and weigh 294 kg each, which may lead to logistical or resource issues if being used to separate beach plastics [26], [45].

2.3.1 Operating Principles

A typical Wilfley table consists of the following elements seen in figure 2 below:

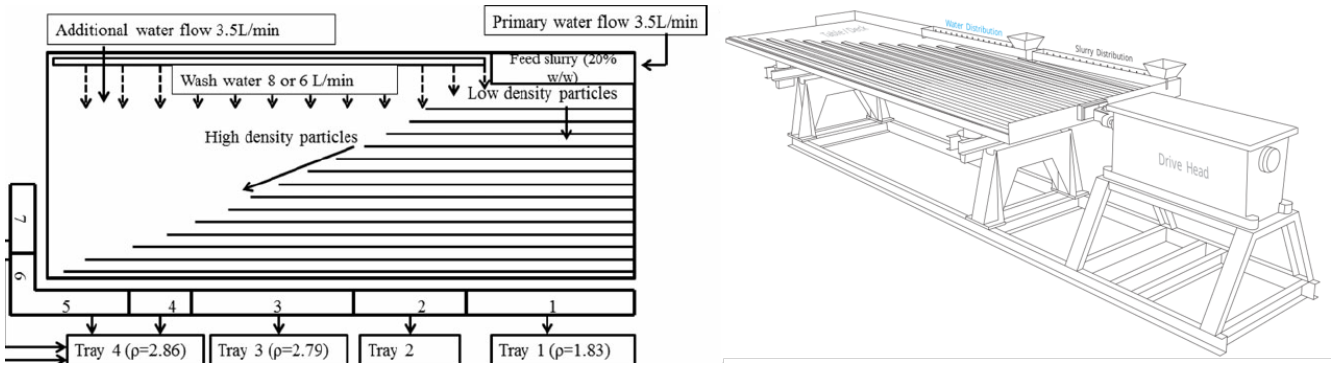


Figure 2: Schematic of Shaking table top (left), oblique section of modern Wilfley table (right) [46][46]

The tabletop is also supported by a stable frame to counteract its oscillation, seen in figure 2 above. A driving mechanism, often mounted on the side, drives an arm which shakes the table along its length. For table operation, raw material is fed into the upper-right end of the table, where particles are carried downwards by both the wash water and deck inclination. This allows material to accumulate in the etched riffle grooves, where they are jogged along the table's length in the right direction by its reciprocating motion [25]. The net effect is a general diagonal movement of particles in the lower-right direction. However, particles of different densities will follow different paths.

As material aggregates within the table grooves, lighter particles will tend to accumulate near the surface as the particulates stratify [47]. These lighter particles, more exposed to wash water, gain buoyancy and are carried downward across the riffles, collecting at the table's bottom edge. Medium-density particles are slightly less affected, being transported along the riffles into the bottom-right table edge. The heaviest particles, usually the target precious metal such as gold, remain largely unaffected by wash water and continue to be jogged to the far-right table edge for deposition. As such, under ideal circumstances, the shaking table is capable of separating a mixed feed of particles into different areas. However, this is under the condition that operating parameters have been fine-tuned to best-fit the input feed.

The operating parameters in question include the stroke length and frequency, material feed rate, deck inclination, table end elevation and wash water flow rate. It is difficult to accurately determine the best possible combination for each feed type as altering a single variable can alter the table's sorting characteristics. As such, RSM experiments are typically required.

2.3.2 Applicability to Microplastic Removal from Sediment

As previously mentioned, shaking tables, once optimised, can achieve considerable separation efficiency for a range of material densities and sizes. Shaking tables are often used to recover silt to coarse sand-sized minerals and precious metals, which is ideal for microplastics removal from beach and river sediment which is of same material size (appendix 6.1). In the context of mineral separation, the densest precious metals are extracted from each feed. In this application, the opposite will be true, extracting the least dense microplastic particulates.

Although shaking tables may be suited to filter sediment and microplastic-sized material, as this is a novel application there is no precedent that separation would be effective. Existing publications on gravity separation suggest that a material's separability is determined by the concentration criterion (CC), defined as [48]:

$$\text{Concentration Criterion} = \frac{\text{Specific Gravity}_{\text{Heavier particle}} - \text{Specific Gravity}_{\text{Wash fluid}}}{\text{Specific Gravity}_{\text{Light particle}} - \text{Specific Gravity}_{\text{Wash fluid}}} \quad (1)$$

Where the specific gravity of a material is its density ratio with respect to fresh water. Ideally, the $CC > 2.5$, which in theory allows separation of particles down to $75\mu\text{m}$ size. For lower CC values, separation is possible but only for larger particles [48]. To apply this to microplastics and sediment, the specific gravity for polymers and CCs are calculated in table 1 below:

Material	Specific Gravity	Concentration Criterion			Separable for sediment size
		Gravel	Sand	Mud	
PP	0.9125	2.92	2.90	3.06	> 0.75 mm
PS	1.005	2.65	2.64	2.78	> 0.75 mm
LDPE	0.93	2.86	2.85	3.00	> 0.75 mm
HDPE	0.96	2.77	2.76	2.91	> 0.75 mm
PVC	1.4	1.90	1.89	1.99	> 1.5 mm
PET	1.38	1.93	1.92	2.02	> 1.5 mm

Table 1: Concentration Criteria calculation for target polymers [49], [50], [51]

To calculate the above CC values, sediment SG is defined as 2.65 (sand), 2.66 (gravel) and 2.79 (mud) [52], [53], [54]. It must be noted that the “separable for size” column relates to the minimum size of sediment which can be removed from the mix, and not the microplastics. Thus for PP, sediments greater than 0.75mm in diameter can, in theory, be removed via Wilfley table. For denser PVC and PET, the minimum separable diameter is 1.5mm. Judging from this, it would be beneficial to develop an artificial sample where sediment is sized 0.75mm and above to reduce material costs.

3 METHODOLOGY

3.1 Aims and Objectives

As previously mentioned, Wilfley tables present a promising new approach to removing microplastics from sediment. However, the method is currently catered towards the mining industry and laboratory use, not suited to microplastics removal where needs differ. Machines are typically expensive, large and immobile, while also requiring specialist operation to ensure efficient separation. A significant portion of plastics removal efforts are completed in small-scale volunteering efforts from non-profit NGOs, with limited capital and logistical resources [55]. As such, this project aim to develop an accessible Wilfley table for microplastic removal. It will aim to satisfy the following requirements:

The table will be small and mobile such that it is transportable without heavy equipment, such as by hand and within personal vehicles. This is to ensure accessibility for volunteer groups operating under low resources. As previously mentioned, much of microplastics removal from public areas is conducted by volunteer groups with logistical capacities typically comprising a van for cleanups [56].

For the same reason, the Wilfley table should be relatively cheap, using only accessible materials. This is to promote accessibility for the table, in both potential application in microplastics removal but also in the case that further research is considered. Ideally, the table will not cost more than £300 at the time of purchase (2024) for prices in London, United Kingdom. This also takes into consideration the budget limitations of this thesis project.

Another aim is that ideally, the table will achieve similar or higher microplastic separability and material throughputs than the existing separation methods for beach and river sediment. Specifically, this is for the most common microplastic polymers of PP, PS, PE, PET and PVC. As this is a novel development, it is understandable that very high separation may not be attainable. However, it is still important to achieve metrics such that the Wilfley table can show promise in this particular application and warrants further research.

Testing and optimisation experiments will be conducted using artificially-spiked sediment. An additional aim is that the fitted model through RSM can accurately depict the relation between operating parameters and the response metrics, allowing for efficient optimisation of parameters. Ideally, the artificial sediment will be accurate enough such that validation experiments see similar recovery results. Ultimately, the overall goal of the project is to provide proof-of-concept research in the feasibility of Wilfley tables for microplastic separation from sediment, and to take strides in developing a practical prototype achieving a balance of effectiveness, accessibility and ease-of-use.

3.2 Artificial Sediment Sample Preparation

As identified in the literature review, the most common plastic sources on rivers and shorelines are PP, PS, PE, PVC and PET. To generate artificial microplastics, popular commercial sources of oceanbound plastic for each polymer were identified, and sourced [14], [57], [58]. These were sourced from everyday items to reduce costs. More sourcing details can be found in appendix 6.2. Care was taken to acquire plastics with a different colour for each polymer, for easier visual identification during sorting. The plastics are then shredded using a 3dEVO SHR3D-IT shredder from the UCL MechSpace, a model which specialises in the required polymers (see appendix 6.3). Shredded polymers are then sorted by size (0-1mm, 1-2mm, 2-3mm, 3-4mm, 4-5mm) using a series of cascading sieves, to ensure a uniform size distribution is present to ensure testing on all-sized material.

It must also be noted that it is difficult to replicate real weathering conditions of microplastics artificially. Practically-sourced microplastics tend to exhibit irregular, pitted and varied topographies, whereas machine-shredded plastics tend to be angular and uniformly shaped [59]. As such, the machine-shredded plastics will likely see increased buoyancies, which will affect/increase/decrease their susceptibility to cross-wash during separation. This highlights the necessity for validation using real sediment, as developed models will likely overfit to the artificial samples used.

In terms of developing artificial river and beach sediment, a number of simplifications were made. As identified by the Udden-Wentworth scale in literature review, the sediment composition includes fine gravel (2-5mm), sand (0.0625-2mm), and muddy silts (<0.0625mm). However, upon reviewing Wilfley table theory, sediments less than 0.75mm in diameter are not separable from the microplastics (table 1). As such, the muddy silts which are at largest 0.0625mm can be omitted to reduce material costs, leaving a gravel and sand mixture.

Also, as identified in literature review, the ratio of sand, gravel and mud can vary greatly by location. This is because shoreline sediment is primarily clastic (fragmented rock), which can have different origins and types [60]. Thus, to ensure different possible sediments are accounted for, a median ratio of 70% sand, 30% gravel is selected to achieve representation of both sand and gravel [61].

3.3 Table Design and Build

Before designing and building specific sections of the table, the general dimensions must be established. Considering the table shape, trapezoidal tables provide higher capacities per table area and improved recovery of finer sized particles [62]. However, they are significantly more complex to produce. Thus, a rectangular shape is considered. For rectangular tables, a length-width ratio between 0.33-0.5 is usually seen, where full-size tables are up to 244x93cm in dimension with 0.38 length-width ratio [26].

It is known that large tabletop areas allow higher material throughputs [47]. However, a design criteria is also to minimise size for mobility. Thus, tabletop dimensions were decided at 80x40cm. This size allows a compromising sorting, whilst becoming significantly easier to transport due to its much smaller footprint and weight. The length-width ratio of 2 was chosen to allow additional deck space for cross wash piping near the table top. This is further discussed in section 3.3.2 below.

This reduced size not only reduces table weight and material volume, increasing mobility and reducing material costs, but also reduces the need for more robust and costlier structural materials. Larger Wilfley tables require steel frames, greatly increasing costs, weight while also making the table less accessible as steel working requires expensive tooling. For this table, softwood and hardwood plywoods were selected as the primary build material. These woods are relatively cheap, and provide a balance of strength and weight while also being accessible and easily workable.

3.3.1 Table Base & Driving Mechanism

With a set general table dimension and material, a suitable supporting frame and driving mechanism must be developed. Typically, shaking tables are driven by a drive head which protrudes from one side of the table, as seen previously in figure 2. The motor drives an eccentric shaft or cam, which is attached to the table top by a linkage arm. As the cam rotates, it forces the deck to slide forward and backward along its long axis, yielding

an almost linear oscillation of the table [62]. However, for this application, a more compact and lightweight design is desired. Ideally, the driving mechanism would be housed underneath the tabletop, mounted on the table base to optimise space.

To this end, three innovative driving mechanisms were considered. The first of which involves attaching an eccentric coupler to a motor mounted on the table base, which translates oscillatory motion to the tabletop through a drive shaft. This design is simple, but lacks a specific attribute. Table driving mechanisms are typically constructed in a way to provide a slow forward stroke, followed by a rapid return stroke. This imbalance promotes the jogging of particles along riffles, enhancing sorting [62]. Seeing as the eccentric coupler provides symmetrical motion for both strokes, this method is unable to satisfy this requirement.

A second method considered uses magnets to generate linear motion. Current is passed through a coil within a magnetic field, producing force via Lorentz's law. An H-bridge circuit alternates the current direction, enabling back-and-forth movement, while pulse width modulation (PWM) can control power delivered to the motor system. This can be controlled using a micro processing unit, adjusting the shaking frequency and amplitude. Despite being a precise and plausible method, the cost of components was expensive, whilst also presenting a fire hazard if contaminated with water. Using this method, the stroke length is also difficult to adjust, and as such may be of use for experiments where stroke length variation is not required.

The final considered system is a hand-cranked version modified from a bicycle gear. This is the most accessible by far but was not chosen due to the immense manual labour needed to continually remove microplastics over time. Ultimately, the first option was selected for its balance of accessibility and effectiveness.

The issue of lacking a stroke speed imbalance was remedied by an innovative support system, comprising four aluminium 1050-grade 3mm-thick sheets acting as flexure supports. Due to their high elasticity, these flexures provide ample structural support for the tabletop, whilst allowing range of motion on one axis for oscillation. To account for the stroke speed imbalance, the flexures are installed such that their elastic energies are loaded against the table motion in one direction. Thus, the forward stroke will be opposed by flexure elasticity, and the return stroke aided by the flexures, bringing about the desired stroke speed imbalance. This combination is attributed to David Roewe, who published his design in the public domain, intended for gold recovery. Permission was granted to use his methods in this project. More details can be found in appendix 6.4.

A prototype was first constructed closely following Roewe's design, with the flexure pieces inserted at a 60° angle from the base (see appendix 6.5). The idea is that jogging motion resulting from the flexures is angled to direct heavier particles towards the lower-right corner for collection. However, it was seen that this angling produced significant stresses to the motor's kinetic chain, as well as the hardwood flexure housing. Thus, the design was simplified as seen in figure 3 below.

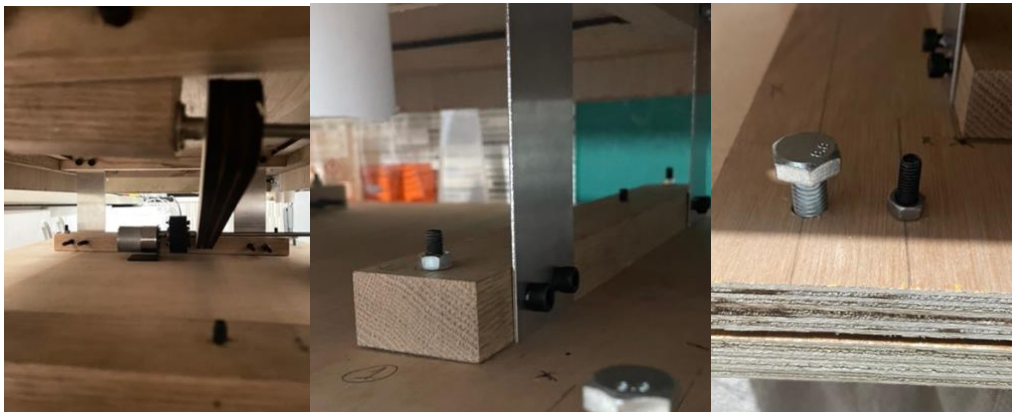


Figure 3: Motor drive system (left), Flexure housing on the table base (middle), and elevation adjustment (right)

Two hardwood plywood pieces of 60x50x1.8cm comprise the table base, and four hardwood 35x2.3x2.5cm frames act as housing points for the flexures. To vary the table's inclination and end elevation, M10 nuts and

bolts are affixed into each corner, allowing each corner to rise and fall along the bolt threads (see figure 3: right). Each corner is accompanied by a smaller M4 fastener pair of nuts and bolts, to affix the table once the desired elevation is reached. Hardwood plywood is selected for its base for its rigidity and weight, as although weight is ideally minimised, a heavier base is required to ensure the table is not too top heavy to cause movement of the base. Hardwood is used in areas requiring high strength, such as in the flexure housings.

For the driving mechanism, a 12V DC motor is fixed to the base via an L-shaped steel mounting bracket. This specific model is used for its low cost, as well as adjustable RPM via PWM. The motor spins an eccentric coupler, improvised by fastening two Delrin (Acetal Homopolymer) circular pieces measuring 5cm in radius and 1cm in thickness. In each of the circular pieces, the entry hole for the 6mm steel shaft is offset according to the desired stroke length, creating the eccentric motion desired as the motor spins. Delrin is selected due to its strength, being able to withstand high torques and stresses whilst also being machinable [63].

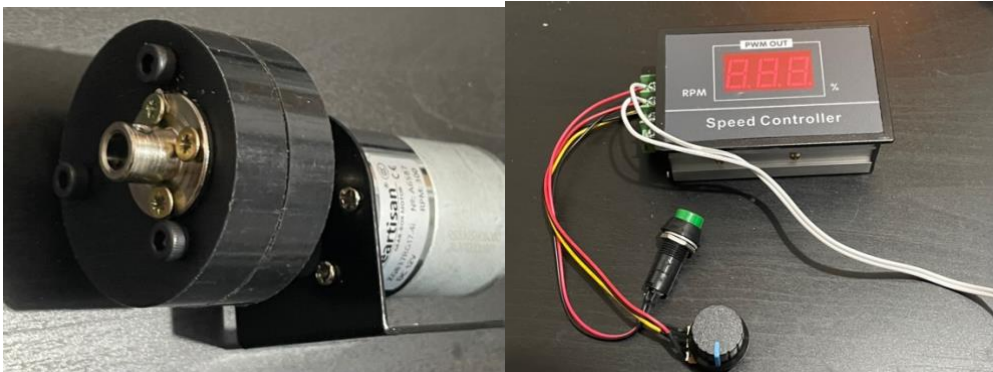


Figure 4: Motor with L-shaped mounting bracket and Delrin eccentric coupler (left), PWM control (right)

3.3.2 Table top and water feed system

The table top is vital to operation, providing a sorting area for material while also splitting material across the table edges and providing cross wash. Ideally, the design makes efficient use of space whilst minimising weight and material cost. The design should also be sturdy to withstand oscillations of up to 300 Hz at 25mm amplitude. A prototype was first developed following typical shaking table convention [62]. This consisted of a 800x400mm sorting space as previously specified.

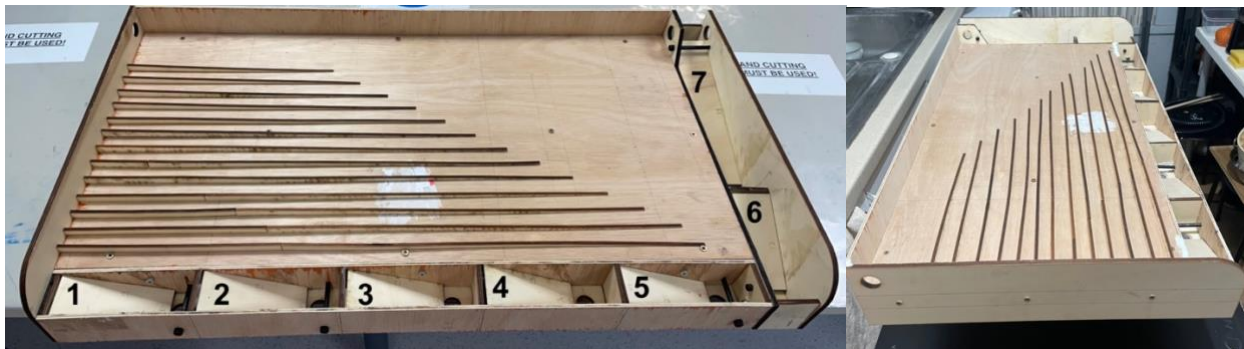


Figure 5: Top (left) and side (right) view of Wilfley table top

The structural frame consists of hardwood beams, providing a sturdy base on which to build the tabletop as well as transferring drive motion from the motor. Although hardwood provides excellent strength, it is dense and expensive. The frame weight and cost is minimised by comprising only a rectangular shape with structural cross-beams.

Peripheral additions such as the splitting bins and the side walls (seen above) are made from softwood plywood and bolstered onto the hardwood frame. The front, side and back walls are necessary to contain splashing water during sorting, and bins necessary of dividing of sorted material. Typically, bins are concentrated on the right-most side, and a single long tailings tray runs along the bottom edge. This is to achieve sorting resolution for denser precious metals, which tend to deposit on the right-most edge. In this application,

sorting resolution is favoured on the bottom edge, where less-dense plastic polymers are expected to wash out. The bins positions are determined as seen in figure 5 above, with 5 bins on the bottom edge and 2 bins on the right edge, numbered 1-7.

To supply cross-wash along the top edge of the table, a 90cm long, 21.5mm-diameter uPVC pipe is used. uPVC is selected over PVC as uPVC lacks plasticisers, making it rigid and less likely to warp when unsupported [64]. The pipe is inserted along a drilled hole on the table's right wall, affixed using epoxy resin. Water is fed into the pipe by sink, using a fastened hosepipe to supply water. To disperse the water evenly along the tabletop, twelve 3 mm diameter holes are drilled along the pipe facing the table's back wall, with an even spacing. Initially, holes were drilled facing downwards, directing water flow directly onto the table. It was noticed that this led to unnecessary splashing, causing rippling and disturbing the uniformity of water across the table. This is undesirable as this may de-stratify material. Thus, the backwards-facing holes directed water onto the back wall, allowing settling of water before travelling across riffles. 2 mm, 2.5 mm and 4 mm diameter holes were also tested for the desired operating flowrates of 1-5 L/min, but it was observed that 3 mm holes exhibited the most even distribution of flow. This is ideal as a uniform flow of cross wash ensures additional forces are not placed onto particles as they collect within table riffles.

Riffle design is also vital to operation, as it directly affects the table's sorting of material. The height of each riffle determines the volume of material which can stratify behind it, while the spacing between successive riffle lines and the individual riffle thicknesses affect the turbulence of water between riffles. Ideally, the water between riffle spaces is "live" enough such that denser sediment is not allowed to completely settle, but currents are strong enough to reject lighter material near the surface. The complete settling of sediment will cause material to stick to the table surface, and may also trap lighter particles within. An effective design can achieve a balance of riffle height, thickness and spacing to facilitate this effect. Riffles are typically approximately 10 mm in height, and cover over half of the table's surface [25], [65]. To encourage ideal vortex patterns between riffles, it is recommended that riffle spacing is approximately double the riffle height [25]. Thus, 10mm heights are separated by 20mm.

During prototype testing, riffles consisted of uniform heights across the entirety of the table. It was seen that plastic pieces discharging over the table's bottom edge were not sorted by density as desired. To facilitate this, the riffles were redesigned to taper off in height along the length of the table, from 10 mm height to 2 mm (see appendix 6.6). This was produced using laser-cutting of softwood plywood sheets to reduce construction time. Thus, as particles jog along the table, the reducing riffle height will gradually expose material to cross wash, leading to a density-gradient along table's bottom edge.

In terms of riffle and tabletop material, shaking tables typically use high coefficient-of-friction surfaces to promote the jogging and stratification of material [25]. As such, materials like neoprene rubber would be ideal. However, this material is not only relatively expensive, but difficult to work with to accurately produce the desired riffle pattern. It was tried as the material for an initial prototype, but was instead substituted for a wooden surface finished with Yacht varnish for waterproofing.

3.4 Parameter Optimisation

Parameter optimisation for shaking tables is a well-studied topic. Shaking tables have six changeable operating parameters, which can all affect the distribution of material across the tabletop. This presents a multi-variable optimisation problem where the optimal combination of parameters is desired, but testing of all possible combinations (full-factorial analysis) would prove too time consuming, requiring $2^6 = 64$ experiments to test only two levels. For such scenarios, design of experiments theory is required, where theory is used to achieve the desired experimental outcome in the lowest number of experiments.

To achieve this, the most common approach used in the context of shaking tables is known as response surface methodology (RSM) [28]. In this method, a system response is designated to score the performance of each set of parameters. For this report, the response is the recovery, separation efficiency, and purity of microplastics, discussed in section 3.5.2 below. Different parameter combinations are then tried, making intentional changes according to RSM experimental design, to identify both the insignificant parameters as well as a response

variable curve with respect to parameters. This allows for fitting of the surface to relate the response to input parameters and determine the local maxima [28].

The two most commonly used variations of RSM are Box-Behnken and Central Composite Design (CCD). Each of these variations employ a slightly different approach to trying parameter combinations, with CCD being more exhaustive, and Box-Behnken favouring efficiency [66], [67]. For the purposes of this report, CCD will be used to provide a more comprehensive understanding of recovery with respect to table parameters. Although, Box-Behnken is recommended if the table is to be used in-field to recover microplastics as it requires fewer experiments.

For experiments with more than 4 factors, CCD and Box-Behnken testing is typically preceded with a screening experiment, to reduce irrelevant factors [68]. This would allow follow-up experiments to increase focus on factors with the largest effect on the system. Screening experiments typically comprise fractional factorial designs, which consider a fraction of the total combinations possible. The degree of reduction is known by resolution, where most resolutions used are between III-V, increasing with resolution [69]. Plackett-Burman (PB) designs are commonly used for screening, and are of resolution III. They specialise in generating economical experiments for cases with high number of factors [70].

Once relevant factors are identified, they can be studied at greater resolution using CCD. CCD involves categorising 2-4 continuous factors into 5 discrete levels: $-\alpha$, -1 , 0 , 1 , $+\alpha$, to allow greater probing into the gradients of the response curve, where α is known as an axial point used to probe the response curve [67]. This allows increased resolution at the cost of increased experimental time. Multiple variations of the method are available. Due to the standard circumscribed variation producing the best results for fitting, it will be used for design of experiment [71]. This will be preceded with a PB screening design for 6 factors.

3.5 Experimental Procedure

3.5.1 Table setup and operation

Before discussing the parameter optimisation method, it is important to explain the table setup and operation, including how parameters are varied. Setup begins at the stroke length, by selecting a Delrin eccentric coupler corresponding to the desired amplitude. Five Delrin couplers were made with varying eccentric holes or each stroke length tested. Between operation, these can be unfastened and replaced to change stroke lengths. The base screws are then turned to raise and lower the table's end elevation and inclination. The resulting angle is determined through simple trigonometry after measuring the raised height for each parameter. Before attaching the sink hosepipe to the table, the water flowrate is first measured using a 1L bucket and recording the time to fill. Different sink flowrates are physically recorded on the knob to ease future adjustments. A hosepipe is then connected between the sink tap and input PVC tube for the table.

Once the motor is turned on, its frequency is variable using a PWM, as a percentage of its maximum RPM (300). Thus, RPMs between 150-300 are achievable in steps of 3 for each percent. Speeds below 150 are not usable seeing as torque is lowered significantly for lower PWM settings [72]. Finally, during operation, material feedrate is varied using (see shaking table paper).

For a particular test, parameters are first set, with the table and water switched on. After the 1L material is exhausted, the table is left to run for 3 minutes for particles to sort. Material left on the table is deemed not separated. This approach to recording results encourages parameters to be optimized also to maximise speed of sorting. Material collected in bins is then removed and separated via visual sorting. This is possible due to the colour-coding of different polymer types. Once manually-separated, they are weighed and thus the corresponding mass of material in each bin can be calculated through its known densities.

3.5.2 Response Metrics

Before considering experimental design, response metrics must be clearly defined to quantify the effectiveness of each experiment. In the mining industry, the most common metrics used are recovery, purity,

and separation efficiency. Recovery quantifies the shaking table's effectiveness in extracting the desired material. In this context, the shaking table's bins 1-5 are defined as fractions for microplastics, where bins 6-7 are for sediment collection. A microplastic recovery is then given by:

$$\text{Microplastic Recovery (\%)} = \frac{\text{mass of microplastics in bins 1 - 5}}{\text{net microplastic mass in feed}} \times 100 \quad (2)$$

Although the recovery is useful for identifying the placement of microplastics, it does not consider any sediment contamination in bins 1-5. The metric would read 100% recovery if all sediment and microplastics deposited into bins 1-5 together. As such, recovery is often used to supplement an effectiveness indicator known as Separation Efficiency (SE), defined as:

$$\text{Separation Efficiency (\%)} = \text{Microplastic Recovery} + \text{Sediment Recovery} - 100\% \quad (3)$$

Where Sediment Recovery is defined as the ratio of sediment mass found in bins 6-7. The SE accounts for both the recovery of target and rejection of unwanted material, and is often used in mineral processing as a single figure of merit [73]. As such, it will be recorded as the primary response metric, as well as the microplastic recovery for reference. A tertiary metric considered is purity, also known as grade, and measures how clean each output stream is. In the context of microplastics, it is measuring the percentage of material found in bins 1-5 that is actually microplastics:

$$\text{Microplastic Fraction Purity} = \frac{\text{mass of microplastics in bins 1 - 5}}{\text{net mass of material (plastics + sediment) in bins 1 - 5}} \times 100 \quad (4)5$$

Although the SE metric is an indicator of the distribution of sediment and microplastics, purity is also an important metric to identify the possible contamination of plastics retrieved. This will be vital if recovered microplastics are chosen to be processed or further refined using smaller-scale methods like density separation.

3.5.3 Plackett-Burman Parameter Screening

A PB design matrix is constructed for 6 factors, seen in appendix 6.7 [70]. It is seen to be highly efficient, requiring only 12 experiments for screening 6 parameters. For each parameter, only high/low values (1/-1) are required. These were intentionally selected to represent the parameter's effect. Values that span a small range may underestimate the effect of the parameter, and the opposite is true [70]. Thus, both the size and density of feed material, as well as typically-used shaking table values were considered when choosing these values.

For table oscillation frequency, shaking tables typically operate at 200-325 Hz, using higher frequencies for finer feeds and vice versa [25], [74]. Feeds can be classified into three categories: coarse (2.0-0.2mm), fine (0.2-0.074mm) and mud (<0.074mm) [75]. For this experiment, feeds are between 0.75-5.0mm, and classified as coarse. As such, the selected frequencies are biased slightly lower, at 200 Hz (low) and 300 Hz (high). In terms of stroke length, 5-25mm lengths are typical, with larger strokes for coarse feeds and vice versa [47]. Following the same principles as above, the chosen values are skewed higher, at 10mm (low), 25mm (high). In terms of deck incline, values between 2.5-9° are typically seen, although a correlation between material properties and incline are not defined [76], [77]. Thus, the full range is used at 2.5° (low), 9° (high). For end elevation (or table slope), a gentle slope is typically included to encourage the jogging of material along the table length. This value typically remains between 1-4° [27][78]. Screening values are selected at 1° (low) and 4° (high).

Cross wash flowrates typically vary greatly between 12-100 L/min, depending on the recovery material and table size [25], [62], [78]. However, experiments with smaller tables have seen much lower flowrates, between 0.05-4 L/min [76]. Due to uncertainties regarding water flowrate, upper and lower bounds were experimentally determined for this specific feed material. The lower bound was determined by a sufficient flow to carry PP, the least dense polymer included. The upper bound is determined by a flow capable of carrying PVC, the most dense polymer. These boundaries were determined at 1 L/min (low) and 5 L/min (high).

A similar process is used to determine the material flowrate, seeing as feed material used in this experiment comprising sediment and microplastics is greatly different to rock and ore used in typical shaking tables, as well as using a smaller tabletop which reduces sorting capacity. Ideally, the feed rate is maximised without allowing material to spill over riffles. An upper bound was defined as just below the rate at which a mix of feed material would spill over riffles on maximum wash flow, and the lower bound determined over the same basis under

minimal wash flow, at 450 g/min and 100 g/min. The PB design matrix is then carried out following the procedures defined in 3.5.1.

3.5.4 Central-Composite Design for Parameter Optimisation

Following the PB screening, it was determined through ANOVA and Pareto chart of standardised effects that Wash Flow rate, Deck Inclination and Feed rate were most significant (discussed in 4.1). A full, 2-block CCD is created for further testing of intervariable effects. The design comprises 20 experiments per repeat, with a default alpha of 1.633. The axial (extreme) points used for parameters in CCD are set to the same extreme values used in PB testing, as both are used to test curvature of inter-factor relations [67], [79].

For the factors deemed insignificant (stroke frequency, stroke length, end elevation), they would remain at a fixed value for the remainder of testing. For this, the regression equation for SE was extracted from the screening experiment to determine the positive or negative effects of parameters. Parameters will then be set to their maximum or minimum correlating to their effects on SE. The CCD design matrix is seen in appendix 6.8 and is then carried out with three repeats.

With data acquired, a model fit can then be applied using Minitab, a data analysis software, allowing for the prediction and optimisation of response metrics using parameter values.

3.5.5 Validation of Predicted Models

Once the fitted models are used to predict an ideal set of parameters, these parameter combinations are experimentally verified using: 1) existing artificial sediment and 2) real sediment and microplastics sourced from the River Thames. For the sourcing of material, recent studies have indicated that sediment in Deptford displays one of the highest microplastic concentrations along the Thames [80]. An accessible foreshore was identified in this area, with postcode SE10 9HT. A temporary river works license was then requested and granted from the Port of London Authority for temporary extraction of sediment material. On site, sediment is extracted through 5mm dry-sieving, extracting both microplastics and sediment of the required size.

Microplastics in the sediment were visually identified and extracted from the sediment by hand, using indicators from existing studies [81], [82]. This allowed for adjustment of the quantities of microplastic present in each sample. The mass concentration of microplastics was identified to be low, at below $0.3 \pm 0.2\%$. Uncertainties stem from the relatively poor accuracy of visual identification. As it would be difficult to visually identify extraction rates for a 0.3% contamination, the sediment quantity was adjusted such that microplastic contamination is 5% by weight.

4 RESULTS AND DISCUSSION

The experiments are carried out, recording the microplastic recovery and SE as response metrics for each experiment. Uncertainties consist of measurement uncertainty found in the scale used, as well as random uncertainty from repeated experiments. They are combined and propagated into calculation for recovery and SE.

4.1 Plackett-Burman Screening

A screening analysis is conducted using Minitab, fitting a model to correlate parameters with response values. The following was investigated in detail to identify significant factors:

4.1.1 Goodness-of-Fit

The model summary seen in table 2 below shows that the fitted values for Microplastic Recovery, Purity and Separation Efficiency exhibit R-squared (R-sq), and in some cases adjusted R-sq and predicted R-sq values. These values provide insight to how well the model fits data and explain variations in responses. For recovery and SE, R-sq values of 87.49% and 76.62% suggest that the model can account for the majority of variability in the target variables, demonstrating a relatively strong fit. This suggests the screening is able to successfully identify key variables for these metrics.

Table 2: Model summary of the PB screening response variables from Minitab

Response	S	R ²	R ² (adj)	R ² (pred)
Microplastic Recovery	6.1455	87.49%	72.48%	27.94%
Microplastic Purity	6.37563	44.24%	0.00%	0.00%
Separation Efficiency	7.5769	76.62%	48.55%	0.00%

However, it is important to note that an R-sq (pred) value of 0.00% indicates overfitting to the data, and no predictive power of the models for Microplastic Purity and Separation Efficiency [83]. This can occur when the model is too complex, fitting random noise or peculiarities in the sample data other than identifying underlying relationships [71]. Although this is undesirable, it is acceptable seeing as values won't be extrapolated from the screening experiment.

4.1.2 Analysis of Variance (ANOVA)

ANOVA analysis is carried out for the screening results, seen in table 3 below. The calculated p-values provide valuable insight into the significance of each parameter onto the corresponding response variable. P-values below 0.05 suggest statistical significance from the factor onto the response variable.

Table 3: Analysis of Variance for PB screening response variables from Minitab

Source	P-value		
	Recovery	Purity	SE
Model	0.036	0.688	0.145
Stroke Length	0.912	0.527	0.589
Stroke Frequency	0.336	0.418	0.298
Wash Flow rate	0.005	0.974	0.024
Deck Inclination	0.024	0.475	0.189
Feed rate	0.793	0.275	0.303
End Elevation	0.599	0.463	0.404

It can be seen that for recovery and SE, significant parameters are wash flowrate and deck inclination. However, for purity, no parameters see p-values below 0.05, likely attributing to its poor fit evidenced by its low R-sq metrics.

4.1.3 Pareto Chart and Mathematical Models

Pareto charts for the recovery and separation efficiency responses are seen below, providing valuable insight into the effects of parameters on response variables. The chart for purity is omitted, seeing as the model fit is poor and will not be used for consideration. The charts display the absolute values of standardised effects in descending order, with a reference line in red for statistical significance at the t-critical value ($\alpha = 0.05$). Values above the line indicate statistical significance, with the bar length correlating to strength of effect on the response variable. The same trends are seen as for p-value analysis, where wash flowrate and deck inclination have the most significant effect.

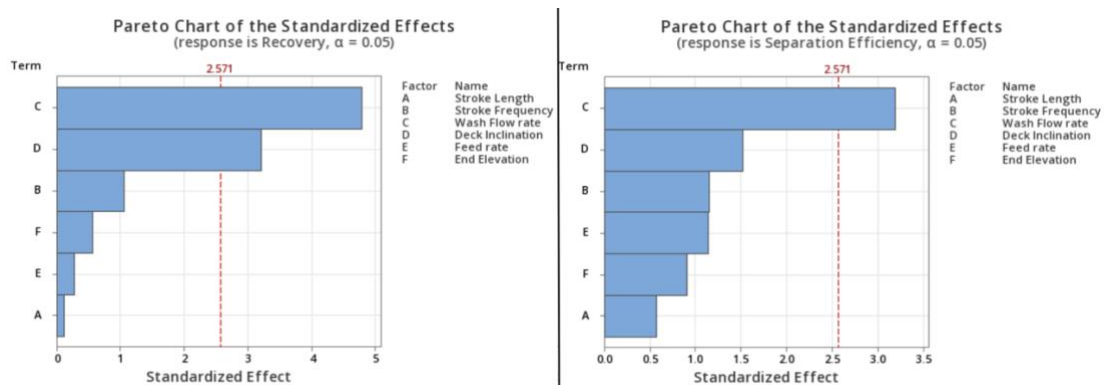


Figure 6: Pareto chart of the standardised effects of screening parameters on Microplastic Recovery (left), Separation Efficiency (right)

The regression equation generated by Minitab for recovery and SE is seen in equation 5,6 below, where factors are denoted A, B, C, D, E, F as in figure 6 above. Similar to previous observations, wash flowrate (C) and deck inclination (D) have the greatest effects, as they have the largest coefficients. It is notable that wash flowrate has a positive effect on recovery and SE, i.e. an increased flow increase response, whereas deck inclination has a negative effect.

$$\text{Recovery} = 54.7 + 0.027A + 0.0378B + 4.262C - 1.755D - 0.0028E - 0.66F \quad (6)$$

$$\text{SE} = 36.0 + 0.168A + 0.0508B + 3.50C - 1.023D - 0.0144E - 1.33F \quad (7)$$

4.1.4 Screening Experiment Conclusions

Throughout sections 4.1.1-4.1.3, a number of statistical tools were used to identify the effects of the table parameters on responses. It is evident that wash flow rate and deck inclination have the greatest effect, and thus are selected for further testing using CCD. The feed rate, despite showing statistical insignificance, is also selected for further testing. This is because an additional success criteria for table operation is material throughput, which ideally is maximised to allow a greater sorting rates of microplastics. Thus, the feed rate is included to further confirm its lack of effects and achieve a maximal sorting rate.

4.2 Parameter Optimisation through Central Composite Design

The CCD experimental design seen in appendix 8 is carried out, and a RSM analysis is carried out in Minitab. Before considering optimisation, a fit analysis is again carried out for verification of significance. During CCD, the factors deemed insignificant during screening are fixed to values based on their positive or negative effects from regression equations 5 and 6. Stroke length is fixed to 25mm, stroke frequency to 300 Hz and end elevation to 1°.

4.2.1 Quality-of-fit Analysis

A model summary is again constructed for the CCD results, showcasing stronger fit values for all response metrics. The relatively high R-sq values of 84.31, 89.46 and 77.00% indicate that the model can adequately explain the variation in each of the response metrics. In addition, the predictive R-sq is 27.67 and 22.33% for recovery and purity, suggesting the model is able to extrapolate values to some extent. However, SE sees a predicted R-sq value of 0.00%, suggesting that the model has again overfit the data [83]. Thus, extrapolating results from the SE model may not yield strong results, as the model has likely overfit on the sample data.

Table 4: Model Summary of the CCD response variables from Minitab

Response	S	R ²	R ² (adj)	R ² (pred)
Microplastic Recovery	8.17249	84.31%	66.87%	27.67%
Microplastic Purity	1.24188	89.46%	77.76%	22.33%
Separation Efficiency	7.17523	77.00%	51.44%	0.00%

An ANOVA analysis for CCD results is also carried out, seen in table 5 below. A similar trend is seen for p-values, where wash flowrate and deck inclination show high significance on recovery and SE. As the fit for purity appears to have improved compared to the PB screening, significance for wash flowrate and deck inclination is also seen. The model's lack-of-fit error is also considered to determine the fit accuracy. This measures the model's inability to fit the data properly. As the p-values for all response metrics are above 0.05, the lack-of-fit is insignificant, suggesting the model fits the data well [71].

Table 5: Analysis of Variance for CCD response variables from Minitab

Source	P-value		
	Recovery	Purity	SE
Model	0.013	0.003	0.056
Wash Flow rate	0.001	0.001	0.002
Feed rate	0.221	0.649	0.303
Deck Inclination	0.007	0.025	0.022
Lack-of-Fit Error	0.831	0.300	0.832

Pareto charts are also again calculated, but did not demonstrate significant inter-factor relations other than wash flow rate and deck inclination. Thus, the charts are omitted from the main text but available in appendix 6.9 for reference. The regression equations determined by Minitab are seen below, this time including purity:

$$\text{Recovery} = 80.1 + 9.6A - 0.157B - 2.81C - 0.88AA - 0.000011BB - 0.362CC + 0.0228AB - 0.04AC + 0.0117BC \quad (8)$$

$$\text{Purity} = 87.78 - 3.47A + 0.0112B + 1.56C + 0.162AA - 0.000011BB - 0.0805CC + 0.00001AB + 0.049AC - 0.00118BC \quad (9)$$

$$\text{SE} = 72.5 + 6.3A - 0.141B - 1.7c - 1.04AA - 0.000009BB - 0.397CC + 0.0211AB + 0.17AC + 0.0110BC \quad (10)$$

In all three models, the analysis reveals that A and C are the most significant, suggesting that for these metrics, wash flowrate and deck inclination are the most significant, with larger effects than any inter-factor relations. This follows the trend seen from PB screening.

The normal probability plots of residuals for the response variables are also generated and plotted, seen below. These plots assess the validity of the assumption that residuals are normally-distributed, as well as the quality of model fit.

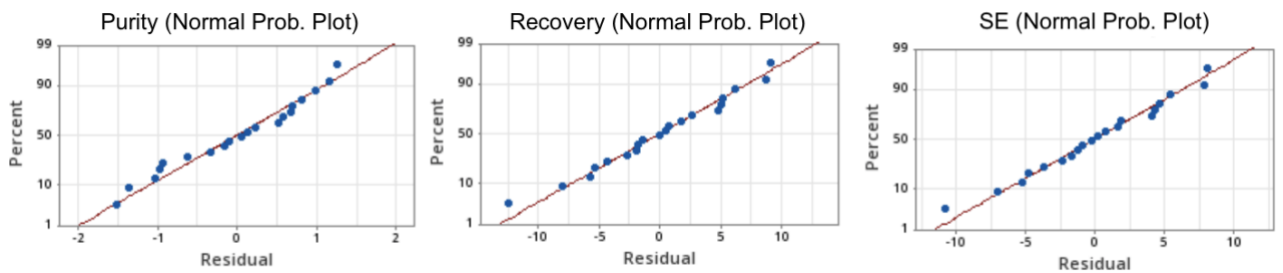
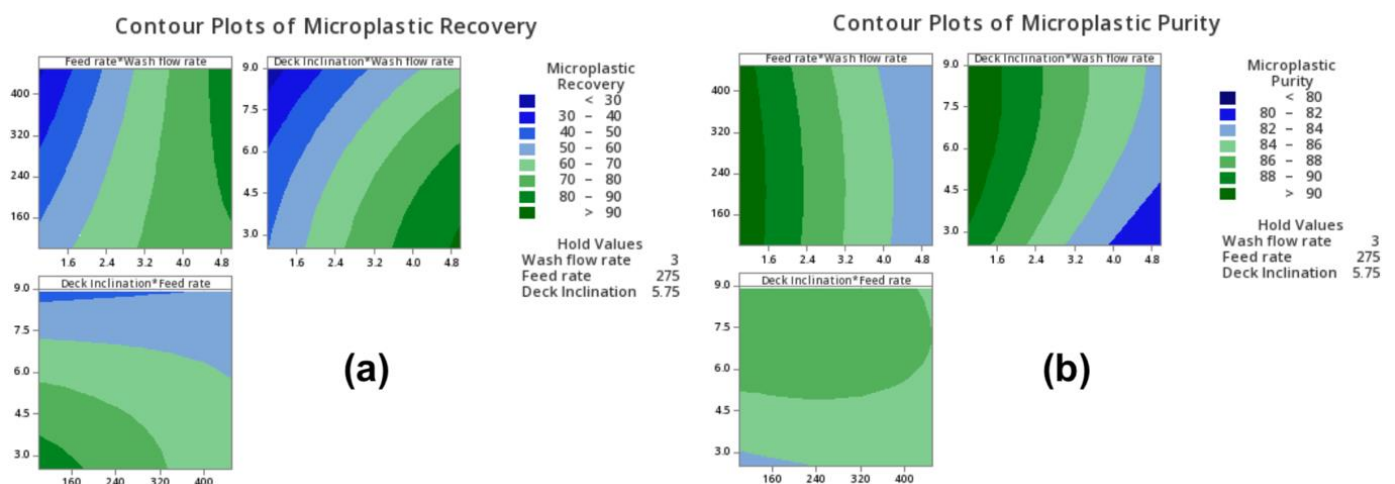


Figure 7: Probability plots of residuals for response variables: microplastic purity (left), recovery (middle), SE (right)

Ideally, data points will align in a straight line, indicating that residuals follow a normal distribution [28]. This is seen to be the case in figure 7, indicating a good model fit. As such, these models are deemed as usable for parameter optimisation.

4.2.2 Contour and Surface Plot of Significant Parameters

To visualise the effect of factors on the response metrics, contour plots of the fitted models were created. These plots demonstrate the relationship between two selected variables, while keeping the remaining variable fixed at their centre value of their experimental range. By analysing these contour plots, researchers can gain deeper insights into how variations in the selected variables affect responses [84]. The visualisation facilitates the identification of optimal parameter settings and helps understand the sensitivity of responses to different variable combinations.



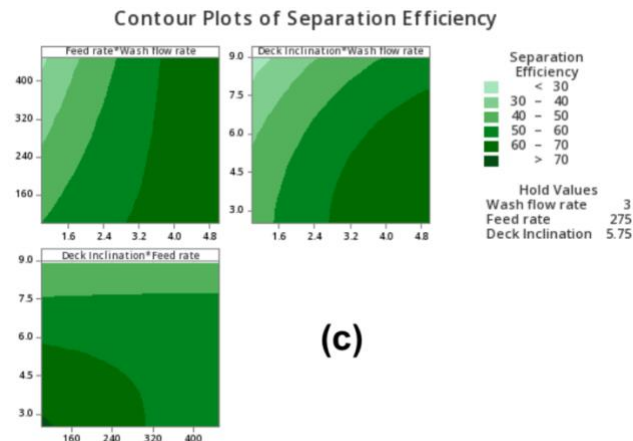


Figure 8: Contour plots of wash flowrate, deck inclination and feed rate for response variables microplastic recovery (a), purity (b) and SE (c)

From figure 8a, it can be seen that optimal results are achieved above 80% recovery. It is evident that higher wash flowrates between 4.0-4.5 L/min provide stronger recovery values, especially in conjunction with a feed rate of 100g/min and 3° inclination. In figure 8b, to attain microplastic purities of above 88%, wash flow rate is minimised to below 1.6 L/min, whilst deck inclination and feed rates are maximised. The contour results for recovery and purity are surprising, seeing as it is expected in theory that increased deck inclination would improve recovery at the cost of purity. However, the opposite is seen in practice, suggesting the influence of additional factors. This could possibly be attributed to turbulence interactions, where high inclinations affect the angling of incoming water into riffles, reducing the effects of hindered settling and allowing particles to settle in riffle gaps. In figure 8c, it can be seen that SE is stronger for low feed rates and deck inclination, in combination with high wash flows. These results adhere more to theory, seeing as reduced feed rates and deck inclination prevent the overspilling of microplastics and sediment over riffles, allowing for accurate sorting.

An overlaid graphical approach is considered in figure 9 below, allowing for visualisation of regions that satisfy specified conditions. The white region within the design space optimisation, known as the “optimised formulation region”, represents the area where desired outcomes are achieved. This chart incorporates all three recovery metrics, as well as all three factors.

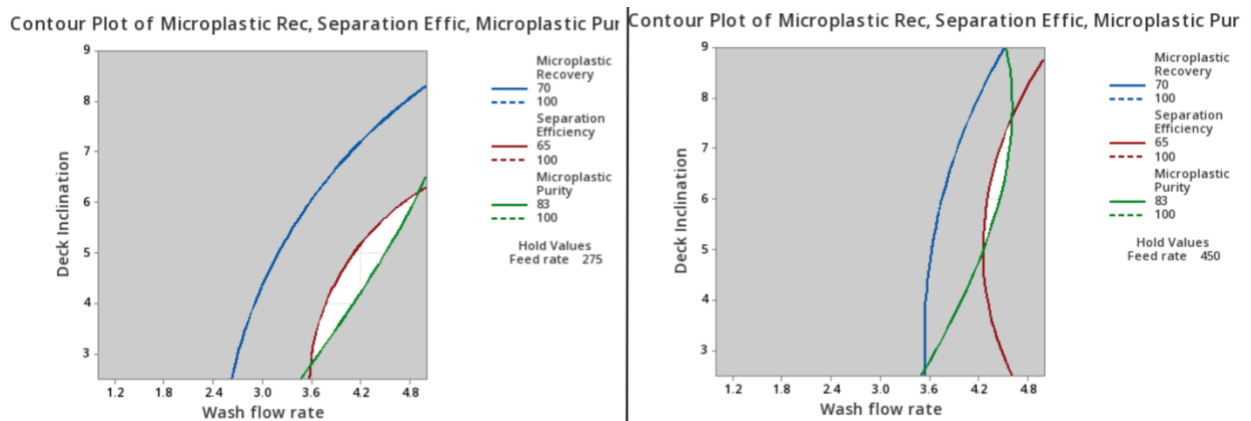


Figure 9: Overlaid contour plots of wash flow rate and deck inclination on microplastic recovery, purity and separation efficiency. Feed rate value is held at 275g/min (left) and 450g/min (right)

Satisfactory conditions are defined as between 70-100% for recovery, 65-100% for SE and 80-100% for purity. The regions highlighted in white are where all three conditions are met. Seeing as feed rate has the lowest statistical significance, it is held at a constant value of 275g/min (left), the centre experiment value, and 450g/min (right), the desired maximum feed rate. It is evident that increasing the feed rate to 450g/min reduces the condition margins but nevertheless, an optimised formulation region is still present, at approximately 4.3-4.5 L/min wash flow and 5.1-7.5° deck inclination.

4.2.3 Predicting Optimum Operating Conditions for Response Metrics

A response optimisation prediction is carried out using Minitab, utilising the developed models for each response to predict the required factor combinations for desired outcomes. The results are seen below in table 6. In the first two rows, all responses are maximised with equal weighting. In the second row, feed rate is affixed to its maximum value of 450 g/min to identify changes in responses under higher material throughputs. Recovery and SE are then prioritised for maximising in the third and fourth rows.

Table 6: Model response predictions under varied optimisation goals, calculated in Minitab

Optimisation Scheme	Factors			Responses			
	Wash flow	Feed rate	Deck Inclination	Recovery	SE	Purity	Composite Desirability
Maximise all	2.25198	100	2.5	79.84%	68.74%	85.19%	0.444129
Maximise all (feed rate: 450g/min)	4.43434	450	6.17677	77.99%	65.79%	83.10%	0.346163
Maximise Recovery	2.9798	100	2.5	85.04%	70.78%	83.37%	0.584285
Maximise SE	2.83818	100	2.5	84.10%	71.16%	83.71%	0.492631

It is evident that the optimiser attempts to reduce wash flow and minimise feed rate and inclination to maximise response variables. This makes sense seeing as slower processing of materials allow more stratification and stable distribution of materials to occur. Although higher inclinations, wash flows and material feed rates can increase a table's material throughput, it is understood that this can lead to excessive turbulence and buildup of material between riffles, reducing the effects of stratification and thus the table's sorting effectiveness. In fixing the feed rate to 450 g/min, the recovery metrics are reduced marginally, ranging from 2.95-1.85% decreases. This is acceptable, seeing as the material throughput is increased by a magnitude of 4.5, verifying previous results noting the relative statistical insignificance of feed rate.

Under the schemes maximising recovery and SE, the responses achieve a peak value of 85.04% and 71.16% respectively, seeing a 7.8% and 8.2% increase compared to the generalised maximisation schemes. These combinations may be considered when a purer sediment or plastic stream is desired.

4.2.4 Validation of Model Predictions

As mentioned in the experimental procedure, the predictions seen in table 6 above will be validated using both existing artificial sediment, as well as real sediment and microplastics extracted from the Thames foreshore. These results are seen in table 7 below.

Table 7: Experimental results for the validation of RSM model using artificial and real sediment

	Optimisation Scheme	Recovery (%)	Recovery (Error %)	SE (%)	SE (Error %)	Purity (%)	Purity (Error %)
Artificial Sediment Validation	Maximise all (feed = 450g/min)	83.615	-7.21	62.173	5.50	85.862	-3.33
	Maximise Recovery	88.194	-3.71	65.775	7.07	76.978	7.67
	Maximise SE	83.427	0.80	75.332	-5.86	85.007	-1.55
Thames Sediment Validation	Maximise all (feed = 450g/min)	66.670	-16.98	48.655	-35.22	63.908	-30.02
	Maximise Recovery	60.014	-41.70	59.751	-18.46	65.796	-26.71
	Maximise SE	61.965	-35.72	50.627	-40.56	62.857	-33.18

In artificial sediment validation, it is seen that the absolute value of error between predicted and validated values are no larger than 8%. This suggests that the CCD RSM is successful in modelling and optimising conditions for this specific experimental setup [85][28]. However, in Thames sediment validation, absolute error ranges up to 42%. This suggests the artificial conditions are unable to replicate real sediment conditions, meaning the fitted model is not applicable to real-world settings. However, the attained recovery, SE and purity

metrics show relative consistency in results, ranging within 9% between the validation experiments. This suggests the separation process is consistent, and optimisation may be possible through CCD using real material.

4.2.5 Polymer Distribution and Recovery

The validation data acquired in table 6 for artificial sediment is used to visualise the distribution of polymers across each bin, seen below. The subplots represent different optimisation schemes, and each line shows the cumulative deposition of material along the table bins. Here, it is seen that lighter polymers like PE and PP skew towards bins 1-3, suggesting they are carried by currents and do not collect in riffles for extended periods of time. Denser plastics like PVC and PET see a more gradual accumulation, mostly collecting across bins 4-6. This is expected as denser plastics are expected to collect and sort along the table riffles.

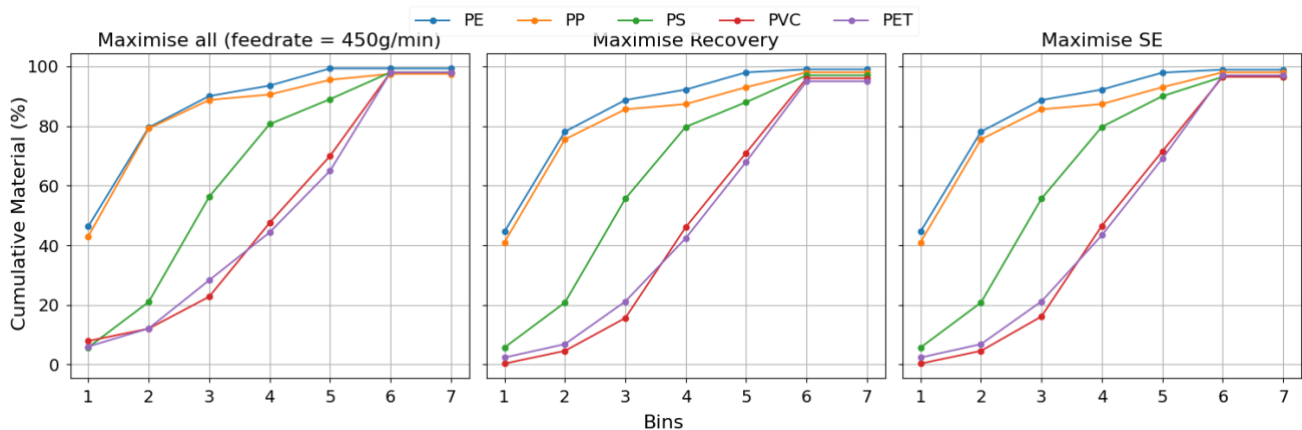


Figure 10: Cumulative distribution of each polymer into bins using validation data from three optimisation schemes

However, it is notable that a significant portion (up to 33%) of denser plastics like PS, PVC and PET collect in bin 6, and thus are not considered recovered as bins 6-7 categorised for sediment collection. This is an expected difficulty, seeing as PET and PVC plastics are known to be difficult to extract due to similar densities with sediment [86]. Thus, if this method is to be applied in-field, multiple passes for material may be required to account for these polymers.

4.3 Discussion

As discussed in section 4.2.4, the developed table design is capable of producing effective and predictable separation on the artificial sediment used, achieving up to 88%, 75%, and 86% for recovery, SE and purity respectively. This is achieved following a 6-factor PB screening experiment, and a follow-up CCD optimisation experiment, for a total of 32 experiments (excluding repeats). Following CCD optimisation, an adequate model was developed relating operating parameters to the response metrics, showcasing R-sq values of between 77-89% correlating to a good model fit. These relations were then used to identify optimum parameter combinations for the desired metrics.

Thus, it is evident that the developed table is capable of replicating the agitation conditions required to facilitate gravity separation. This was done while ensuring the table is relatively cheap and lightweight, allowing for the avoiding of logistical issues which otherwise would be faced when using a full-size shaking table in this application. The table costs £289 (excluding screws, tools and glues required which were sourced from UCL MechSpace, and prototyping costs), with the full list of purchases seen in appendix 6.10. This is a fraction of the price of commercial Wilfley tables, which often range between £1,500-30,000 depending on size [45]. In addition, the developed table is significantly more mobile, weighing just 22kg, opposed to metal laboratory tables which typically weigh 300 kg [26]. The table is also easily collapsible, as the aluminium flexures used can be unscrewed to separate the tabletop and base, allowing for easier transportation.

In comparison with existing methods such as density separation, the shaking table method is able to achieve 88% and 67% SE on artificial and real sediment respectively, compared to 93-98% recovery seen for density

separation using NaCl [87]. NaCl solutions are selected for comparison as they are the most scalable medium, being cheap, accessible and environmentally-friendly. Although density separation can achieve higher recoveries, NaCl (1.2 g cm^{-3}) is unable to remove denser plastics like PET and PVC, and thus is unable to address a significant portion of plastics. These plastics are often found in river sediment, due to their lack of capacity for long-distance transport by water [88]. In addition, the achieved 450 g/min of feed material far exceeds throughput capacities seen in density separation. In typical laboratory-scale extractions, density separation requires 2 hours of settling time for a 400ml sample, although larger scales have been seen at 5-6kg sediment per run, requiring 24 hours settling time [40], [89], [42].

It must also be addressed that strong recovery metrics seen in artificial sediment validation do not translate to that of real sediments, seeing relative reductions of up to 42% for responses. This is understandable, seeing as real sediment contains a heterogeneous mix of materials, including organic matter like shell fragments, wood/seaweed, or dried algae [86]. As such, pre-treatments such as chemical digestion are typically seen in laboratory extraction to improve recovery rates [86]. In addition, as previously mentioned, the buoyancy characteristics of weathered and machine-produced microplastics can vary greatly, where real microplastics can sometimes develop biofilm coatings and break into polydisperse fragments [59]. Weathered pieces with biofouling can also behave effectively heavier, which may allow them to settle like sediment particles, reducing separability. As such, further studies are recommended to acquire large quantities of weathered plastics and sediment for parameter modelling.

In addition, it was also observed that material would often become wedged within riffle grooves, leading to a net loss of approximately 2-3% material per experiment, as the wedged material was wiped clean between each test for consistency. Excessive material buildup between riffles may alter the table's sorting characteristics to some extent, and thus should be avoided where possible, especially during optimisation testing. As such, in future table builds, it is recommended to smooth out sharp angles in the riffle spaces to avoid material buildup, possibly through the use of epoxy putty. For future considerations, a water recirculation system would also be desired to allow in-field operation for the table. As it stands, the table is mobile but requires a stationary water supply, restricting table's logistics. Water re-feeding systems capable of tolerating Wilfley table feed are expensive, and can increase a commercial table's price by up to £2,000 [45], [90]. As such, research into developing an accessible recirculation system would be highly desirable.

5 CONCLUSION

Ultimately, in this report, an accessible, low-cost shaking table is developed for the removal of microplastics from sediment, achieving up to 88% recovery and 75% separation efficiency on the tested artificial material. Although microplastic and sediment compositions and distributions are researched to develop a representative artificial testing sample, validation on real microplastics and sediment extracted from the River Thames yielded weaker results at 67% recovery and 60% separation efficiency. However, the goal of developing an accessible, mobile shaking table unit for microplastics recovery from sediment is still ultimately achieved. To extend the table's applicability to real sediment, further optimisation research is recommended using real microplastics and sediment.

6 APPENDIX

Millimeters (mm)	Micrometers (μm)	Phi (ϕ)	Wentworth size class
4096		-12.0	Boulder
256		-8.0	Cobble
64		-6.0	Pebble
4		-2.0	Granule
2.00		-1.0	Very coarse sand
1.00		0.0	Coarse sand
1/2	0.50	1.0	Medium sand
1/4	0.25	2.0	Fine sand
1/8	0.125	3.0	Very fine sand
1/16	0.0625	4.0	Coarse silt
1/32	0.031	5.0	Medium silt
1/64	0.0156	6.0	Fine silt
1/128	0.0078	7.0	Very fine silt
1/256	0.0039	8.0	Clay
0.00006	0.06	14.0	Mud

Appendix 6-1: Udden-Wentworth scale for classification of sediment [91]

	Polymer				
	PE	PP	PS	PET	PVC
Product types	Shampoo/soap containers	Bottle caps	Plastic cutlery	Soft drink bottles	Pipes
	Ketchup / sauce bottles	Lunch boxes	Food containers	Fibres	Toys
	Packaging wrap	Laboratory consumables	Foam packaging	Thin films	Garden hoses

Appendix 6-2: Microplastic polymers and common commercial product applications [14], [57], [58]



Appendix 6-3: Shredded microplastic samples for PET in green, and PS in white (left). 3dEVO SHR3D-IT microplastic shredder (right)

Appendix 6-4: David Roewe contact information

David Roewe was kind enough to publish his Wilfley table designs and ideas to the public domain for use. Permission was requested and granted to utilise portions of his designs. He can be contacted at orophilia@gmail.com.



Appendix 6-5: Pictures of prototype build following David Roewe's flexure design



Appendix 6-6: Tapered side profile of riffle design

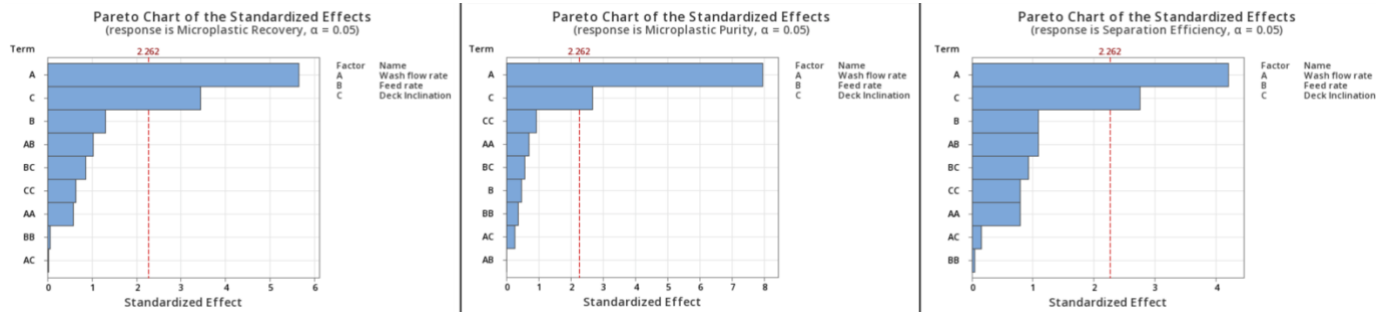
Run Order	Stroke Length [mm]	Stroke Frequency [Hz]	Wash water flowrate [L/min]	Deck Inclination [°]	End Elevation [°]	Material Feed rate [g/min]
1	10	200	1	9	4	450
2	25	200	1	2.5	4	450
3	10	200	1	2.5	1	100
4	25	200	5	9	4	100
5	25	300	5	2.5	4	450
6	10	300	1	2.5	4	100
7	10	300	5	2.5	1	450
8	25	300	1	9	1	100
9	10	200	5	9	1	450
10	25	300	1	9	1	450
11	25	200	5	2.5	1	100
12	10	300	5	9	4	100

Appendix 6-7: Uncoded experiment design for 12-experiment, 6-factor Plackett-Burman screening

Run Order	Wash water flowrate [L/min]	Material Feed rate [g/min]	Deck Inclination [°]
1	3	275	9
2	3	100	5.75
3	3	275	5.75
4	1	275	5.75
5	3	275	2.5
6	3	450	5.75
7	5	275	5.75
8	3	275	5.75
9	4.22474	167.835	7.7402
10	3	275	5.75
11	1.77526	167.835	3.7598
12	4.22474	167.835	3.7598
13	4.22474	382.165	7.7402
14	4.22474	382.165	3.7598
15	1.77526	382.165	3.7598

16	1.77526	167.835	7.7402
17	3	275	5.75
18	1.77526	382.165	7.7402
19	3	275	5.75
20	3	275	5.75

Appendix 6-8: Uncoded experiment design for 20-experiment, 3-factor Central Composite Design



Appendix 6-9: Pareto charts of response metrics for CCD Optimisation

Materials	Items/equipment	Hazardous Materials
Hardwood plywood sheet 60x60x1.8cm	Flange couplers for 6mm motor steel shaft	JB-Weld Epoxy Resin
Hardwood planed timber 240x2.6x4.5cm	Mini DC Motor L-mounting bracket	Water Epoxy Putty
Hardwood plywood 122x60x0.5cm	Mini DC Motor 12V 300-RPM	
Hardwood plywood 80x40x0.5cm	Plastic outdoor water hose pipe 25mm diameter with fastener	
PVC pipe push-stop 21.5mm diameter	Insulated copper wiring	
uPVC waste pipe 21.5mm diameter	PWM DC Motor Controller	
PVVC pipe elbow 21.5mm diameter	12V Power supply	
Gravel 2-5mm size		
Sand 0-2mm size		
1050-grade Aluminium sheets 15x15x0.5cm (x2)		
Delrin (Acetal Homopolymer) rod, 30cm leng, 5cm diameter		

Appendix 6-10: Table of materials & items used in build. For hazardous materials, safety sheets are referenced and adhered to before use

7 REFERENCES

- [1] 'OECD Data Explorer - Archive • Plastics use by application'. Accessed: Feb. 07, 2025. [Online]. Available: [https://data-explorer.oecd.org/vis?tenant=archive&df\[ds\]=DisseminateArchiveDMZ&df\[id\]=DF_PLASTIC_USE_10&df\[ag\]=OECD&lom=LASTNPERIODS&lo=5&to\[TIME_PERIOD\]=false](https://data-explorer.oecd.org/vis?tenant=archive&df[ds]=DisseminateArchiveDMZ&df[id]=DF_PLASTIC_USE_10&df[ag]=OECD&lom=LASTNPERIODS&lo=5&to[TIME_PERIOD]=false)
- [2] R. Geyer, J. R. Jambeck, and K. L. Law, 'Production, use, and fate of all plastics ever made', *Sci. Adv.*, vol. 3, no. 7, p. e1700782, Jul. 2017, doi: 10.1126/sciadv.1700782.
- [3] P. P. Prabhu, K. Pan, and J. N. Krishnan, 'Microplastics: Global occurrence, impact, characteristics and sorting', *Front. Mar. Sci.*, vol. 9, Sep. 2022, doi: 10.3389/fmars.2022.893641.

- [4] S. Ghosh, J. K. Sinha, S. Ghosh, K. Vashisth, S. Han, and R. Bhaskar, 'Microplastics as an Emerging Threat to the Global Environment and Human Health', *Sustainability*, vol. 15, no. 14, Art. no. 14, Jan. 2023, doi: 10.3390/su151410821.
- [5] 'Plastic Pollution - Our World in Data'. Accessed: Feb. 07, 2025. [Online]. Available: <https://ourworldindata.org/plastic-pollution?insight=plastic-production-has-more-than-doubled-in-the-last-two-decades#key-insights>
- [6] S. Karbalaei, P. Hanachi, T. R. Walker, and M. Cole, 'Occurrence, sources, human health impacts and mitigation of microplastic pollution', *Environ. Sci. Pollut. Res.*, vol. 25, no. 36, pp. 36046–36063, Dec. 2018, doi: 10.1007/s11356-018-3508-7.
- [7] Z. Akdogan and B. Guven, 'Microplastics in the environment: A critical review of current understanding and identification of future research needs', *Environ. Pollut.*, vol. 254, p. 113011, Nov. 2019, doi: 10.1016/j.envpol.2019.113011.
- [8] L. Lebreton *et al.*, 'Evidence that the Great Pacific Garbage Patch is rapidly accumulating plastic', *Sci. Rep.*, vol. 8, no. 1, p. 4666, Mar. 2018, doi: 10.1038/s41598-018-22939-w.
- [9] J. L. Conkle, C. D. Báez Del Valle, and J. W. Turner, 'Are We Underestimating Microplastic Contamination in Aquatic Environments?', *Environ. Manage.*, vol. 61, no. 1, pp. 1–8, Jan. 2018, doi: 10.1007/s00267-017-0947-8.
- [10] H.-X. Li *et al.*, 'Microplastics contamination in bivalves from the Daya Bay: Species variability and spatio-temporal distribution and human health risks', *Sci. Total Environ.*, vol. 841, p. 156749, Oct. 2022, doi: 10.1016/j.scitotenv.2022.156749.
- [11] R. Mkuye *et al.*, 'Effects of microplastics on physiological performance of marine bivalves, potential impacts, and enlightening the future based on a comparative study', *Sci. Total Environ.*, vol. 838, p. 155933, Sep. 2022, doi: 10.1016/j.scitotenv.2022.155933.
- [12] Y. M. Lozano, C. A. Aguilar-Trigueros, G. Onandia, S. Maaß, T. Zhao, and M. C. Rillig, 'Effects of microplastics and drought on soil ecosystem functions and multifunctionality', *J. Appl. Ecol.*, vol. 58, no. 5, pp. 988–996, 2021, doi: 10.1111/1365-2664.13839.
- [13] A. A. de Souza Machado *et al.*, 'Microplastics Can Change Soil Properties and Affect Plant Performance', *Environ. Sci. Technol.*, vol. 53, no. 10, pp. 6044–6052, May 2019, doi: 10.1021/acs.est.9b01339.
- [14] A. I. Osman *et al.*, 'Microplastic sources, formation, toxicity and remediation: a review', *Environ. Chem. Lett.*, vol. 21, no. 4, pp. 2129–2169, Aug. 2023, doi: 10.1007/s10311-023-01593-3.
- [15] A. A. Mamun, T. A. E. Prasetya, I. R. Dewi, and M. Ahmad, 'Microplastics in human food chains: Food becoming a threat to health safety', *Sci. Total Environ.*, vol. 858, p. 159834, Feb. 2023, doi: 10.1016/j.scitotenv.2022.159834.
- [16] C. Campanale, C. Massarelli, I. Savino, V. Locaputo, and V. F. Uricchio, 'A Detailed Review Study on Potential Effects of Microplastics and Additives of Concern on Human Health', *Int. J. Environ. Res. Public Health*, vol. 17, no. 4, Art. no. 4, Jan. 2020, doi: 10.3390/ijerph17041212.
- [17] M. A. Browne *et al.*, 'Accumulation of Microplastic on Shorelines Worldwide: Sources and Sinks', *Environ. Sci. Technol.*, vol. 45, no. 21, pp. 9175–9179, Nov. 2011, doi: 10.1021/es201811s.
- [18] H. S. Carson, S. L. Colbert, M. J. Kaylor, and K. J. McDermid, 'Small plastic debris changes water movement and heat transfer through beach sediments', *Mar. Pollut. Bull.*, vol. 62, no. 8, pp. 1708–1713, Aug. 2011, doi: 10.1016/j.marpolbul.2011.05.032.
- [19] L. Lebreton, M. Egger, and B. Slat, 'A global mass budget for positively buoyant macroplastic debris in the ocean', *Sci. Rep.*, vol. 9, no. 1, p. 12922, Sep. 2019, doi: 10.1038/s41598-019-49413-5.
- [20] M. Rani *et al.*, 'A Complete Guide to Extraction Methods of Microplastics from Complex Environmental Matrices', *Molecules*, vol. 28, no. 15, p. 5710, Jul. 2023, doi: 10.3390/molecules28155710.
- [21] A. Bellasi, G. Binda, A. Pozzi, G. Boldrocchi, and R. Bettinetti, 'The extraction of microplastics from sediments: An overview of existing methods and the proposal of a new and green alternative', *Chemosphere*, vol. 278, p. 130357, Sep. 2021, doi: 10.1016/j.chemosphere.2021.130357.
- [22] N. Stile *et al.*, 'Extraction of microplastic from marine sediments: A comparison between pressurized solvent extraction and density separation', *Mar. Pollut. Bull.*, vol. 168, p. 112436, Jul. 2021, doi: 10.1016/j.marpolbul.2021.112436.

- [23] S. J. F. F. Ramage *et al.*, 'Rapid extraction of high- and low-density microplastics from soil using high-gradient magnetic separation', *Sci. Total Environ.*, vol. 831, p. 154912, Jul. 2022, doi: 10.1016/j.scitotenv.2022.154912.
- [24] B. A. Wills, 'CHAPTER 10 - GRAVITY CONCENTRATION', in *Mineral Processing Technology (Fourth Edition)*, B. A. Wills, Ed., in International Series on Materials Science and Technology. , Amsterdam: Pergamon, 1988, pp. 377–419. doi: 10.1016/B978-0-08-034937-4.50019-3.
- [25] M. A. Silva, *Placer Gold Recovery Methods*. Division of Mines and Geology, 1986.
- [26] 'Products - Holman Wilfley'. Accessed: Feb. 18, 2025. [Online]. Available: <https://www.holmanwilfley.co.uk/products/>, <https://www.holmanwilfley.co.uk/products/>
- [27] D. A. R. Mackay *et al.*, 'Concentration of carbonatite indicator minerals using a Wilfley gravity shaking table: a case history from the Aley carbonatite, British Columbia, Canada', *Geol. Fieldwork 2014 Br. Columbia Minist. Energy Mines Br. Columbia Geol. Surv. Pap. 2015-1*, pp. 189–195, Jan. 2015.
- [28] R. H. Myers, D. C. Montgomery, and C. M. Anderson-Cook, *Response Surface Methodology: Process and Product Optimization Using Designed Experiments*. John Wiley & Sons, 2016.
- [29] Z. Yuan, R. Nag, and E. Cummins, 'Ranking of potential hazards from microplastics polymers in the marine environment', *J. Hazard. Mater.*, vol. 429, p. 128399, May 2022, doi: 10.1016/j.jhazmat.2022.128399.
- [30] OECD, *Global Plastics Outlook: Economic Drivers, Environmental Impacts and Policy Options*. OECD, 2022. doi: 10.1787/de747aef-en.
- [31] P. G. C. Nayanathara Thathsarani Pilapitiya and A. S. Ratnayake, 'The world of plastic waste: A review', *Clean. Mater.*, vol. 11, p. 100220, Mar. 2024, doi: 10.1016/j.clema.2024.100220.
- [32] 'Plastic product lifespans by type', Statista. Accessed: Feb. 08, 2025. [Online]. Available: <https://www.statista.com/statistics/1357773/plastic-product-lifespans-by-type/>
- [33] Y. Li, H. Zhang, and C. Tang, 'A review of possible pathways of marine microplastics transport in the ocean', *Anthr. Coasts*, vol. 3, no. 1, pp. 6–13, Jan. 2020, doi: 10.1139/anc-2018-0030.
- [34] M. Hoseini and T. Bond, 'Predicting the global environmental distribution of plastic polymers', *Environ. Pollut. Barking Essex 1987*, vol. 300, p. 118966, May 2022, doi: 10.1016/j.envpol.2022.118966.
- [35] G. Erni-Cassola, V. Zadjelovic, M. I. Gibson, and J. A. Christie-Oleza, 'Distribution of plastic polymer types in the marine environment; A meta-analysis', *J. Hazard. Mater.*, vol. 369, pp. 691–698, May 2019, doi: 10.1016/j.jhazmat.2019.02.067.
- [36] 'Plastiglomerate - Journal #78'. Accessed: Feb. 19, 2025. [Online]. Available: <https://www.e-flux.com/journal/78/82878/plastiglomerate/#>
- [37] '23 Million Pounds of Plastic Removed From Beaches in Unprecedented Cleanup', Global Citizen. Accessed: Feb. 19, 2025. [Online]. Available: <https://www.globalcitizen.org/en/content/international-coastal-cleanup-report/>
- [38] M. Hoseini and T. Bond, 'Predicting the global environmental distribution of plastic polymers', *Environ. Pollut. Barking Essex 1987*, vol. 300, p. 118966, May 2022, doi: 10.1016/j.envpol.2022.118966.
- [39] A. Bellasi, G. Binda, A. Pozzi, G. Boldrocchi, and R. Bettinetti, 'The extraction of microplastics from sediments: An overview of existing methods and the proposal of a new and green alternative', *Chemosphere*, vol. 278, p. 130357, Sep. 2021, doi: 10.1016/j.chemosphere.2021.130357.
- [40] T. Langknecht *et al.*, 'Comparison of two procedures for microplastics analysis in sediments based on an interlaboratory exercise', *Chemosphere*, vol. 313, p. 137479, Feb. 2023, doi: 10.1016/j.chemosphere.2022.137479.
- [41] 'A new approach in separating microplastics from environmental samples based on their electrostatic behavior - ScienceDirect'. Accessed: Feb. 19, 2025. [Online]. Available: <https://www.sciencedirect.com/science/article/abs/pii/S0269749117316548>
- [42] M. B. Zobkov and E. E. Esiukova, 'Evaluation of the Munich Plastic Sediment Separator efficiency in extraction of microplastics from natural marine bottom sediments', *Limnol. Oceanogr. Methods*, vol. 15, no. 11, pp. 967–978, 2017, doi: 10.1002/lom3.10217.
- [43] T. R. Strong and R. L. Driscoll, 'A process for reducing rocks and concentrating heavy minerals', U.S. Geological Survey, 2016–1022, 2016. doi: 10.3133/ofr20161022.
- [44] A. Falconer, 'Gravity Separation: Old Technique/New Methods', *Phys. Sep. Sci. Eng.*, vol. 12, no. 1, p. 812865, 2003, doi: 10.1080/1478647031000104293.

- [45] 'Gold Shaker Tables - 911Metallurgist'. Accessed: Feb. 18, 2025. [Online]. Available: <https://www.911metallurgist.com/equipments/shaker-tables/>
- [46] D. Palakkeel Veetil, G. Mercier, J.-F. Blais, and M. Chartier, 'Remediation of Contaminated Dredged Sediments Using Physical Separation Techniques', *Soil Sediment Contam. Int. J.*, vol. 23, Apr. 2014, doi: 10.1080/15320383.2013.783556.
- [47] M. C. Fuerstenau and K. N. Han, *Principles of Mineral Processing*. SME, 2003.
- [48] A. Gupta and D. Yan, Eds., 'Chapter 16 - Gravity Separation', in *Mineral Processing Design and Operations (Second Edition)*, Amsterdam: Elsevier, 2016, pp. 563–628. doi: 10.1016/B978-0-444-63589-1.00016-2.
- [49] G. Wypych, 'PS polystyrene', in *Handbook of Polymers*, G. Wypych, Ed., Oxford: Elsevier, 2012, pp. 541–547. doi: 10.1016/B978-1-895198-47-8.50162-4.
- [50] N. P. Cheremisinoff, 'P', in *Condensed Encyclopedia of Polymer Engineering Terms*, N. P. Cheremisinoff, Ed., Boston: Butterworth-Heinemann, 2001, pp. 200–255. doi: 10.1016/B978-0-08-050282-3.50021-4.
- [51] 'GESTIS-Stoffdatenbank'. Accessed: Feb. 19, 2025. [Online]. Available: <https://gestis.dguv.de/data?name=530566&lang=en>
- [52] C. MacRobert and L. A. Torres-Cruz, 'Evaluation of methods to determine reference void ratios', 2016, pp. 255–260. doi: 10.1201/b21335-46.
- [53] B. Prakash, Kulkarni, and P. Nemade, 'Evaluation of Experimental Datasets on Physical properties of Natural Sands and Crushed Sand', Jan. 2020.
- [54] A. Hosni, N. Pauzi, and A. Sharif-fuddin, 'Geotechnical Properties of Waste Soil from Closed Construction Dumping Area in Serdang, Selangor, Malaysia', *Electron. J. Geotech. Eng.*, vol. 20, Sep. 2015.
- [55] 'Beach Cleanups', Surfrider Foundation. Accessed: Feb. 19, 2025. [Online]. Available: <https://cleanups.surfrider.org/about/beach-cleanups/>
- [56] 'River clean-ups', Thames21. Accessed: Feb. 19, 2025. [Online]. Available: <https://www.thames21.org.uk/river-foreshore-clean-ups/>
- [57] F. Uran *et al.*, 'Significance of Plastic Recycling with the Focus on Polyesters - Creating a Circular Economy', *Chimia*, vol. 77, pp. 836–841, Dec. 2023, doi: 10.2533/chimia.2023.836.
- [58] D. T. Kuok Ho, 'Abundance and Distribution of Microplastics in the Water and Riverbank Sediment in Malaysia - A Review', *Biointerface Res. Appl. Chem.*, vol. 11, pp. 11700–11712, Jan. 2021, doi: 10.33263/BRIAC114.1170011712.
- [59] S. Kefer, O. Miesbauer, and H.-C. Langowski, 'Environmental Microplastic Particles vs. Engineered Plastic Microparticles—A Comparative Review', *Polymers*, vol. 13, no. 17, p. 2881, Aug. 2021, doi: 10.3390/polym13172881.
- [60] R. Huggett, *Fundamentals of Geomorphology*, 2nd ed. London: Routledge, 2007. doi: 10.4324/9780203947111.
- [61] H. wan mohtar, S. Bassa, and M. Porhemmat, 'Grain Size Analysis of Surface Fluvial Sediments in Rivers in Kelantan, Malaysia', *Sains Malays.*, vol. 46, pp. 685–693, May 2017, doi: 10.17576/jsm-2017-4605-02.
- [62] 'Gold Shaking Table - 911Metallurgist'. Accessed: Feb. 13, 2025. [Online]. Available: <https://www.911metallurgist.com/blog/gold-shaking-tables/>
- [63] T. Boissonneault, 'Delrin material properties, applications, and more'. Accessed: Feb. 19, 2025. [Online]. Available: <https://www.wevolver.com/article/delrin-material>
- [64] 'Differences Between PVC And UPVC | Ctube'. Accessed: Feb. 19, 2025. [Online]. Available: <https://www.ctube-gr.com/news/differences-between-upvc-and-pvc.html#>
- [65] M. B. McClenaghan, 'Overview of common processing methods for recovery of indicator minerals from sediment and bedrock in mineral exploration', *Geochem. Explor. Environ. Anal.*, vol. 11, pp. 265–278, Dec. 2011, doi: 10.1144/1467-7873/10-IM-025.
- [66] '5.3.3.6.2. Box-Behnken designs'. Accessed: Feb. 19, 2025. [Online]. Available: <https://www.itl.nist.gov/div898/handbook/pri/section3/pri3362.htm>
- [67] '5.3.3.6.1. Central Composite Designs (CCD)'. Accessed: Feb. 16, 2025. [Online]. Available: <https://www.itl.nist.gov/div898/handbook/pri/section3/pri3361.htm>
- [68] '5.3.3.4.6. Screening designs'. Accessed: Feb. 19, 2025. [Online]. Available: <https://www.itl.nist.gov/div898/handbook/pri/section3/pri3346.htm>

- [69] '5.3.3.4.4. Fractional factorial design specifications and design resolution'. Accessed: Feb. 19, 2025. [Online]. Available: <https://www.itl.nist.gov/div898/handbook/pri/section3/pri3344.htm>
- [70] R. L. PLACKETT and J. P. BURMAN, 'THE DESIGN OF OPTIMUM MULTIFACTORIAL EXPERIMENTS', *Biometrika*, vol. 33, no. 4, pp. 305–325, Jun. 1946, doi: 10.1093/biomet/33.4.305.
- [71] D. Montgomery and C. St, *Design and Analysis of Experiments, 9th Edition*. 2022.
- [72] 'Pulse Width Modulation for Power Converters: Principles and Practice | IEEE eBooks | IEEE Xplore'. Accessed: Feb. 19, 2025. [Online]. Available: <https://ieeexplore.ieee.org/book/5264450>
- [73] S. N. F, 'Separation Efficiency, Society of Mining Engineer', *AIME*, vol. 247, pp. 81–87, 1970.
- [74] R. H. (Robert H. Richards, *Textbook of ore dressing*. New York and London, McGraw-Hill Book Company, Inc., 1940. Accessed: Feb. 13, 2025. [Online]. Available: <http://archive.org/details/atextbookoredre00richgoog>
- [75] 'Complete Guide of Gold Shaking Table - Xinhai'. Accessed: Feb. 13, 2025. [Online]. Available: <https://www.xinhaimining.com/newp/complete-guide-of-gold-shaking-table.html>
- [76] R. Razali and T. J. Veasey, 'Statistical modelling of a shaking table separator part one', *Miner. Eng.*, vol. 3, no. 3, pp. 287–294, Jan. 1990, doi: 10.1016/0892-6875(90)90124-T.
- [77] R. J. Manser, R. W. Barley, and B. A. Wills, 'The shaking table concentrator — The influence of operating conditions and table parameters on mineral separation — The development of a mathematical model for normal operating conditions', *Miner. Eng.*, vol. 4, no. 3, pp. 369–381, Jan. 1991, doi: 10.1016/0892-6875(91)90142-I.
- [78] W. Dahani, B. Patty, S. Subandrio, and E. Budhya, 'USE OF GOOD TABLE ("WILFLEY TABLE" TECHNIQUE) AS A BENEFFIATION OF GOLD CARRIER MINERALS', *PETROJurnal Ilm. Tek. Perminyakan*, vol. 8, p. 75, Jul. 2019, doi: 10.25105/petro.v8i2.4780.
- [79] '5.3.3.5. Plackett-Burman designs'. Accessed: Feb. 16, 2025. [Online]. Available: <https://www.itl.nist.gov/div898/handbook/pri/section3/pri335.htm>
- [80] M. M. Trusler, V. L. Moss-Hayes, S. Cook, B. H. Lomax, and C. H. Vane, 'Microplastics pollution in sediments of the Thames and Medway estuaries, UK: Organic matter associations and predominance of polyethylene', *Mar. Pollut. Bull.*, vol. 208, p. 116971, Nov. 2024, doi: 10.1016/j.marpolbul.2024.116971.
- [81] G. Nandikes, O. Banerjee, M. Mirthipati, A. Bhargavi, H. Jones, and P. Pathak, 'Separation, Identification, and Quantification of Microplastics in Environmental Samples', in *Microplastic Pollutants in Biotic Systems: Environmental Impact and Remediation Techniques*, vol. 1482, in ACS Symposium Series, no. 1482, vol. 1482. , American Chemical Society, 2024, pp. 1–19. doi: 10.1021/bk-2024-1482.ch001.
- [82] V. Hidalgo-Ruz, L. Gutow, R. C. Thompson, and M. Thiel, 'Microplastics in the marine environment: a review of the methods used for identification and quantification', *Environ. Sci. Technol.*, vol. 46, no. 6, pp. 3060–3075, Mar. 2012, doi: 10.1021/es2031505.
- [83] A. Gelman, B. Goodrich, J. Gabry, and A. Vehtari, 'R-squared for Bayesian Regression Models', *Am. Stat.*, vol. 73, no. 3, pp. 307–309, Jul. 2019, doi: 10.1080/00031305.2018.1549100.
- [84] L. Panda, P. K. Banerjee, S. K. Biswal, R. Venugopal, and N. R. Mandre, 'Modelling and optimization of process parameters for beneficiation of ultrafine chromite particles by selective flocculation', *Sep. Purif. Technol.*, vol. 132, pp. 666–673, Aug. 2014, doi: 10.1016/j.seppur.2014.05.033.
- [85] J. Frost, *Regression Analysis: An Intuitive Guide for Using and Interpreting Linear Models*. Statistics by Jim Publishing, 2020.
- [86] M. Rani *et al.*, 'A Complete Guide to Extraction Methods of Microplastics from Complex Environmental Matrices', *Molecules*, vol. 28, no. 15, p. 5710, Jul. 2023, doi: 10.3390/molecules28155710.
- [87] M. Scheurer and M. Bigalke, 'Microplastics in Swiss Floodplain Soils', *Environ. Sci. Technol.*, vol. 52, no. 6, pp. 3591–3598, Mar. 2018, doi: 10.1021/acs.est.7b06003.
- [88] A. Haque, T. M. Holsen, and A. B. M. Baki, 'Distribution and risk assessment of microplastic pollution in a rural river system near a wastewater treatment plant, hydro-dam, and river confluence', *Sci. Rep.*, vol. 14, no. 1, p. 6006, Mar. 2024, doi: 10.1038/s41598-024-56730-x.
- [89] T. W. Crutchett and K. R. Bornt, 'A simple overflow density separation method that recovers >95% of dense microplastics from sediment', *MethodsX*, vol. 12, p. 102638, Jun. 2024, doi: 10.1016/j.mex.2024.102638.

- [90] 'Gold Shaker Table Gemini Table'. Accessed: Feb. 19, 2025. [Online]. Available: <https://www.ukumbagold.co.za/shakertable/>
- [91] J. A. UDDEN, 'Mechanical composition of clastic sediments', *GSA Bull.*, vol. 25, no. 1, pp. 655–744, Jan. 1914, doi: 10.1130/GSAB-25-655.